



# Surface-circulation change in the Southern Ocean across the Middle Eocene Climatic Optimum: inferences from dinoflagellate cysts and biomarker paleothermometry

5

Marlow J. Cramwinckel<sup>1</sup>, Lineke Woelders<sup>1,\*</sup>, Emiel P. Huurdeman<sup>2</sup>, Francien Peterse<sup>1</sup>, Stephen J. Gallagher<sup>3</sup>, Jörg Pross<sup>2</sup>, Catherine E. Burgess<sup>4,#</sup>, Gert-Jan Reichert<sup>1,5</sup>, Appy Sluijs<sup>1</sup>, Peter K. Bijl<sup>1</sup>

<sup>1</sup>Department of Earth Sciences, Faculty of Geoscience, Utrecht University, Utrecht, The Netherlands

10 <sup>2</sup>Paleoenvironmental Dynamics Group, Institute of Earth Sciences, Heidelberg University, Heidelberg, Germany

<sup>3</sup>School of Earth Sciences, The University of Melbourne, Melbourne, Australia

<sup>4</sup>School of Earth and Ocean Sciences, Cardiff University, Cardiff, United Kingdom

<sup>5</sup>NIOZ Royal Netherlands Institute for Sea Research and Utrecht University, Den Burg, Texel, The Netherlands

\*Now at Institute of Arctic and Alpine Research, University of Colorado, Boulder, US

15 #Now at Shell UK LTD, Aberdeen, UK

*Correspondence to:* Marlow J. Cramwinckel ([m.j.cramwinckel@uu.nl](mailto:m.j.cramwinckel@uu.nl))

## Abstract

Global climate cooled from the early Eocene hothouse (~52–50 Ma) to the latest Eocene (~34 Ma). At the same time, the tectonic evolution of the Southern Ocean was characterized by the opening and deepening of circum-Antarctic gateways, which affected both surface- and deep-ocean circulation. The Tasman Gateway played a key role in regulating ocean throughflow between Australia and Antarctica. Southern Ocean surface currents through and around the Tasman Gateway have left recognizable tracers in the spatiotemporal distribution of plankton fossils, including organic-walled dinoflagellate cysts. This spatiotemporal distribution depends on physico-chemical properties of the water masses in which these organisms thrived. The degree to which the geographic path of surface currents (primarily controlled by tectonism) or their physico-chemical properties (significantly impacted by climate) have controlled the composition of the fossil assemblages has, however, remained unclear. In fact, it is yet poorly understood to what extent oceanographic response as a whole was dictated by climate change, independent of tectonics-induced oceanographic changes that operate on longer time scales.

To disentangle the effects of tectonism and climate in the southwest Pacific Ocean, we target a climatic deviation from the long-term Eocene cooling trend, a 500 thousand year long global warming phase termed the Middle Eocene Climatic Optimum (MECO; ~40 Ma). The MECO warming is unrelated to regional tectonism, and thus provides a test case to investigate the oceans physiochemical response to climate change only. We reconstruct changes in surface-water circulation and temperature in and around the Tasman Gateway during the MECO through new palynological and organic geochemical records from the central Tasman Gateway (Ocean Drilling Program Site 1170), the Otway Basin (southeastern Australia) and the Hampden Section (New Zealand). Our results confirm that dinocyst communities track tectonically driven circulation patterns, yet the variability within these communities can be driven by superimposed temperature change. Together with

35



published results from the east of the Tasman Gateway, our results suggest that as surface-ocean temperatures rose, the East Australian Current extended further southward during the peak of MECO warmth. Simultaneous with high sea-surface temperatures in the Tasman Gateway area, pollen assemblages indicate warm temperate rainforests with paratropical elements along the southeastern margin of Australia. Finally, based on new age constraints we suggest that a regional  
5 southeast Australian transgression might have been caused by sea-level rise during MECO.

## 1 Introduction

The Eocene epoch (~56–34 millions of years ago; Ma) was characterised by gradual ocean cooling from the early Eocene hothouse (~52–50 Ma) into the early Oligocene icehouse (33 Ma), accompanied by decreasing atmospheric CO<sub>2</sub> concentrations (Zachos et al., 2008; Inglis et al., 2015; Anagnostou et al., 2016; Cramwinckel et al., 2018). In the framework  
10 of Eocene climate evolution, the Southern Ocean (SO) and its circulation are of particular interest. Geochemical tracers (Thomas et al., 2003; Huck et al., 2017) and model simulations using specific Eocene boundary conditions (Huber and Caballero, 2011) indicate that the SO, and the Southwest Pacific (SWP) in particular (Sijp et al., 2014; Baatsen et al., 2018), was the main source of intermediate-deep water formation during the early Paleogene. This effectively relays SO surface conditions to the global deep ocean. However, several sites from the SWP sector of the SO have yielded proxy-based sea-  
15 surface temperatures (SSTs) (Bijl et al., 2009; Hollis et al., 2009, 2012) that are 5–10°C higher than the temperatures derived from the current generation of fully coupled climate models (Huber and Caballero, 2011; Lunt et al., 2012; Cramwinckel et al., 2018). These high marine-based temperatures are supported by vegetation-based temperature estimates on the surrounding continents that indicate paratropical conditions (Carpenter et al., 2012; Pross et al., 2012; Contreras et al., 2013, 2014). This proxy-model mismatch has remained a conundrum.

20

As a result of tectonic processes the bathymetry and geography of the Southern Ocean experienced major reorganizations in the Eocene (Cande and Stock, 2004; Kennett et al., 1974) that strongly affected (global) ocean circulation (Huber et al., 2004; Sijp et al., 2014) (**Figure 1**). In the earliest Eocene, the Australian and South American continents were much closer to Antarctica (e.g., Cande and Stock, 2004) and obstructed circum-Antarctic ocean circulation. Instead, sub-polar gyres  
25 dominated circulation patterns in the southern sectors of the Indian and Pacific Ocean, transporting relatively warm surface waters to the Antarctic coast (Huber et al., 2004; Sijp et al., 2011; Baatsen et al., 2018) (**Figure 1a**). Tectonic activity in the Eocene led to the opening and subsequent deepening of the Tasman Gateway (Bijl et al., 2013b; Stickley et al., 2004b) and Drake Passage (Lagabriele et al., 2009; Scher and Martin, 2004), a transition from northwesterly to accelerated northerly displacement of the Australian continent (Cande and Stock, 2004; Hill and Exon, 2004; Williams et al., 2019), post-rift  
30 collapse of the outer continental shelf on both the Australian and Antarctic margins (Close et al., 2009; Totterdell et al., 2000), and complex paleobathymetric change of the partially submerged continent Zealandia and the Lord Howe Rise in the Tasman Sea related to the initiation of subduction (Sutherland et al., 2017, 2018). This complex tectonic evolution should



have reoriented oceanographic and possibly also atmospheric circulation, and redistributed heat and salinity, regions of deep-water formation, and moisture.

Along with the indirect inferences of modelling and heat distribution based on SST reconstructions, biogeographic patterns of surface-water plankton may be used as a tool to reconstruct surface-ocean circulation. In the Paleogene Southern Ocean, high levels of endemism to the circum-Antarctic region characterise a diverse suite of fossil assemblages, including molluscs (Zinsmeister, 1979), radiolarians and diatoms (Harwood, 1991; Lazarus et al., 2008; Pascher et al., 2015; Stickley et al., 2004b), calcareous nannoplankton and planktonic foraminifera (Nelson and Cooke, 2001; Villa et al., 2008), and organic dinoflagellate cysts (dinocysts) (Wrenn and Beckman, 1982; Wrenn and Hart, 1988; Bijl et al., 2011, 2013a). The endemic dinocyst assemblage from the Southern Ocean is traditionally referred to as “Transantarctic Flora” (Wrenn and Beckman, 1982) (here: Antarctic endemic dinocysts) and has been shown to track Antarctica-derived surface currents, while cosmopolitan assemblages track currents sourced from the low latitudes (Huber et al., 2004; Warnaar et al., 2009; Bijl et al., 2011, 2013b). Throughout the Eocene, the Australian margin of the Australo-Antarctic Gulf (AAG) as well as New Zealand in the Tasman Sea were characterised by high percentages of cosmopolitan dinocysts, implying an influence of the low-latitude-sourced Proto-Leeuwin Current (PLC) and the East Australian Current (EAC), respectively (**Figure 1**). In contrast, coeval assemblages on the eastern side of the Tasman gateway were Antarctic-endemic, showing influence of the Antarctica-derived northward-flowing Tasman Current (TC) (Bijl et al., 2011, 2013b; Huber et al., 2004). From about ~50 Ma onwards, endemic dinocysts assemblages were established on both the Antarctic margin in the Australo-Antarctic Gulf and the eastern boundaries of the Tasman Gateway and Drake Passage (Bijl et al., 2011, 2013b). This indicates surficial westward flow through the Tasman Gateway of a proto-Antarctic Counter Current (proto-ACC), which is supported by simulations using an intermediate-complexity coupled model (Sijp et al., 2016). Pronounced widening and deepening of the gateway did not start until the late Eocene (Stickley et al., 2004b), although some subsidence already took place during the middle Eocene (Röhl et al., 2004).

These biogeographical patterns broadly confirm the Paleogene ocean circulation patterns as simulated by numerical climate models (Huber et al., 2004). Thus, on tectonic timescales (i.e., tens of Myrs), plankton biogeographical patterns predominantly follow changes in surface-ocean circulation (cf. Bijl et al., 2011). During periods with a relatively stable ocean-current configuration, such as the middle Eocene, SO dinocyst assemblage variability was instead driven by (orbital-scale; Warnaar et al., 2009) climatic factors such as SST (cf. Bijl et al., 2011). Superimposed changes in SWP dinocyst assemblages also occur during transient climate change events such as the Paleocene-Eocene Thermal Maximum (PETM, ~56 Ma, (Sluijs et al., 2011)) and the Middle Eocene Climatic Optimum (MECO, ~40 Ma, (Bijl et al., 2010)). The MECO was a 500 thousand year (kyr) period of transient deep-ocean (Bohaty et al., 2009; Bohaty and Zachos, 2003) and widespread surface-water (Boscolo-Galazzo et al., 2014; Cramwinckel et al., 2018) warming of approximately 4–6°C, and global perturbations in ocean environments (e.g., Spofforth et al., 2010; Sluijs et al., 2013; Boscolo-Galazzo et al., 2015;



Cramwinckel et al., 2019). At the East Tasman Plateau, the MECO is characterised by an incursion of low-latitude dinocyst taxa that temporarily replaced the largely endemic Antarctic community (Bijl et al., 2010). The origin of these cosmopolitan dinocysts remains an outstanding question. Potentially, cosmopolitan dinoflagellates outcompeted the Antarctic-endemic taxa in the warming TC. Alternatively, a southward extension of the EAC from the north or leakage of the PLC from the west through the Tasmanian Gateway supplied cosmopolitan assemblages to the region east of Tasmania. In addition, the mechanism that caused MECO warming remains enigmatic. Deep-ocean carbonate dissolution (Bohaty et al., 2009), indications for  $p\text{CO}_2$  rise (Bijl et al., 2010) and a diminished weathering feedback (van der Ploeg et al., 2018) during the MECO imply that climate change was forced by an accumulation of volcanic carbon in the exogenic carbon pool. One of the proposed MECO carbon-cycle scenarios suggests a global sea-level rise in order to shift the locus of carbonate deposition from the deep ocean to the continental shelves (Sluijs et al., 2013). Although speculative isotopic evidence for a MECO-associated change in glacioeustasy exists (Dawber et al., 2011), data from marginal marine sites to assess global sea level change during the MECO are lacking.

To disentangle the effects of tectonism and climate change in the southwest Pacific Ocean, we here assess the biotic and oceanographic response in that region to MECO warming. The MECO allows us to assess oceanographic response to climate change, independent of tectonic-induced change. We reconstruct surface-ocean circulation and temperature by generating new dinocyst and organic geochemical records from Ocean Drilling Program (ODP) Site 1170 on the South Tasman Rise in the central Tasman Gateway. We place these records into their broader regional context by comparing them to newly generated middle Eocene palynological records, including pollen from terrestrial plants, from the Otway Basin (SE Australia) and the Hampden Section (New Zealand) (**Figure 2a**).

## 2 Material

### 2.1 South Tasman Rise (ODP Site 1170) and East Tasman Plateau (ODP Site 1172)

Ocean Drilling Program Site 1170 is located at a water depth of  $\sim 2704$  m, 400 km south of Tasmania at  $47.1507^\circ$  S and  $146.0498^\circ$  E (Exon et al., 2001) (**Figure 2a**). It was drilled on the western side of the South Tasman Rise (STR), a continental block to the south of present-day Tasmania. The site is located in a 2–3 km deep and 50 km wide graben of the Ninene Basin (**Figure 2b**). A  $\sim 300$  m thick package of shallow marine silty claystones of middle Eocene age overlies an erosional unconformity. Northwest-southeast rifting between Australia and Antarctica accelerated after 51 Ma, resulting in prominent NW-SE structural trends in seabed seismic topography associated with seafloor spreading between Tasmania-STR on the one side and Antarctica on the other (Bijl et al., 2013b; Exon et al., 2004; Williams et al., 2019) (**Figure 2a**). This coincided with renewed subsidence of both conjugate continental margins (Totterdell et al., 2000) and the STR (Hill and Exon, 2004). Marked lateral thinning of middle Eocene deposits at Site 1170 is apparent in the seismic profile, suggesting syndepositional growth faulting caused local subsidence (**Figure 2c**). Middle Eocene sediments are present in



Hole 1170D as a thick sequence from ~500 metre below sea floor (mbsf) to the total depth at 780 mbsf (Exon et al., 2001). The precise age of the middle Eocene strata at Site 1170 has thus far not been well constrained (Stickley et al., 2004a). Nevertheless, the thickness of the middle Eocene sequence implies high sedimentation rates ( $\geq 10$  cm/kyr), together with the seismic evidence suggesting that the surrounding graben was a depocenter that formed as rifting developed. Middle Eocene  
5 sediments are overlain by latest Eocene-earliest Oligocene glauconite-rich clayey siltstones (Exon et al., 2001; Sluijs et al., 2003; Stickley et al., 2004a). Here, we target the middle Eocene claystones from the interval ~500–780 mbsf for dinocyst biogeography and organic geochemistry, to gain a central Tasman Gateway perspective on regional effects of the MECO.

Ocean Drilling Program Site 1172 is located at a water depth of ~2620 m on thinned continental crust on the western side of  
10 the East Tasman Plateau (ETP), ~170 km southeast of Tasmania at 43.9598° S and 149.9283° E (Exon et al., 2001). While the ETP has a similar tectonic history to the STR, Site 1172 was not affected by growth faulting and subsidence like Site 1170 during the middle Eocene (Hill and Moore, 2001). Palynological and organic geochemical results for the middle Eocene of the East Tasman Plateau are presented in Bijl et al. (2009, 2010, 2011, 2013a), and are compared to our results from the South Tasman Rise in this study.

15

## 2.2 Latrobe-1 borehole, Otway Basin (Australo-Antarctic Gulf, Southeast Australia)

Sediment cores from the Otway Basin, on the Australian margin of the AAG (**Figure 2a**), were analysed as a location under influence of the PLC during the MECO interval. The Otway Basin contains a regionally thick sequence of shallow-marine Paleogene deposits (Gallagher et al., 1999; Gallagher and Holdgate, 2000). These deposits developed due to Paleocene-  
20 Eocene post-rift extension on the edge of the continental margin, causing subsidence of extensive troughs that served as depocentres of terrigenous sediment in deltaic and shallow marine environments (Krassay et al., 2004; Stacey et al., 2013; Frieling et al., 2018a). In southeast Australia, the middle Eocene to early Oligocene Nirranda Group unconformably overlies the early Eocene Dilwyn Formation (Wanggerip Group) (Abele, 1994; Krassay et al., 2004; Tickell et al., 1993). This unconformity can be traced throughout southeast Australia (Holdgate et al., 2003). The overlying Wilson Bluff transgression  
25 has an age between 44 and 40 Ma (Holdgate et al., 2003; McGowran et al., 2004). In the Portland Trough and Port Campbell Embayment of the Otway Basin, the basal part of the Nirranda Group consists mainly of the Burrungule and Sturgess Point members. Outside of these main depocentres and on the ridges in between, the basal part of the Nirranda Group is represented by the Narrawaturk formation. Planktonic foraminiferal biostratigraphy indicates a Bartonian age for the Sturgess Point Member (Abele, 1994; Gallagher and Holdgate, 2000).

30

We have studied the Latrobe-1 borehole, which covers the top-Wanggerip unconformity and overlies the basal Nirranda group near the Port Campbell Embayment depocenter. The Latrobe-1 core (38.693009° S, 143.149995° E) was drilled in 1963–1964 and reached a total depth of 620 metres. It spans Cretaceous to Eocene sediments, with initial biostratigraphic



age constraints (Archer, 1977; Taylor, 1964; Tickell et al., 1993) and well log data (White, 1963) placing the middle Eocene Narrawaturk Fm at a depth of 60–76 metres below surface (mbs), overlying the Dilwyn Fm (76–289 mbs). The Dilwyn Fm in the Latrobe-1 core consists largely of light- to dark-brown sandstones with some contributions of mud- and siltstone, while the Narrawaturk Fm is a dark brown muddy sandstone (Frieling et al., 2018a). Based on the occurrence of the stratigraphic marker dinocysts *Achilleodinium biformoides* and *Dracodinium rhomboideum*, and in accordance with the regional dinocyst zonation (Bijl et al., 2013a) sediments around a depth of 67.35 metres below surface (mbs) in the Narrawaturk formation (Nirranda Group) of the Latrobe-1 borehole have an age near the MECO (Frieling et al., 2018a). Here, we target the Latrobe-1 core Narrawaturk Fm and top Dilwyn Fm (interval ~60-90 mbs) for palynology and organic geochemistry.

10

### 2.3 Hampden Beach section (South Island, New Zealand)

The Hampden section at Hampden Beach, New Zealand (**Figure 2a**) (45.30° S, 170.83° E) was analysed as a pre-MECO New Zealand end-member, which could have recorded influences of both TC and/or EAC (Hines et al., 2017). Middle Eocene sediments of the Hampden section consist of calcareous clay-rich siltstone to very fine sandstone. Benthic foraminiferal assemblages suggest a depositional environment near the shelf-slope transition. An interval of 4 m was previously selected for high-resolution investigation (Burgess et al., 2008). This interval spans 70 kyr around 41.7 Ma, based on biostratigraphy and orbital interpretation of lithological cycles. Sea-surface temperature (SST) reconstructions based on Mg/Ca and  $\delta^{18}\text{O}$  of excellently preserved foraminifera and  $\text{TEX}_{86}$  indicate values of 23–25 °C (Burgess et al., 2008). We have analysed the same 4 m interval for dinocyst biogeography.

## 20 3 Methods

### 3.1 Palynology

#### 3.1.1 Processing and analysis

A total of 43 samples from ODP Site 1170 (Hole 1170D), eight samples from the Latrobe-1 core, and 39 samples from the Hampden section were processed for palynology following standard procedures. A known amount of *Lycopodium clavatum* spores was added for quantification of the dinocyst content. Sediment samples were crushed and oven dried (60 °C), followed by treatment with 30% HCl and ~40% HF to dissolve carbonate and silicate minerals, respectively. After each acid step, samples were washed with water, centrifuged or settled for 24 h, and decanted. The residue was sieved over nylon mesh sieves of 250  $\mu\text{m}$  and 10  $\mu\text{m}$  (Site 1170) or 15  $\mu\text{m}$  (Otway Basin, Hampden Section) and subjected to an ultrasonic bath to break up agglutinated particles of the residue. A drop of the homogenised residue was mounted on a glass microscope slide with glycerine jelly and sealed. All slides are stored in the collection of the Laboratory of Palaeobotany and Palynology,

30



Utrecht University. Palynomorphs were counted up to a minimum of 200 identified dinocysts for ODP Site 1170. Because the dinocyst yield was relatively low for the other localities, palynomorphs were counted up to a minimum of 90 (Hampden Section) or 50 (Otway Basin) identified dinocysts. Terrestrial palynomorphs were counted in broad categories of gymnosperm pollen, angiosperm pollen and spores for Site 1170 and the Hampden Section. As the Otway Basin samples yielded diverse and abundant sporomorph assemblages, a minimum of 300 sporomorphs was counted per sample. Dinocyst taxonomy as cited in Williams et al. (2017) was generally followed, with the exception of the Wetzellioid family, for which the suggestions made in Bijl et al. (2016) were followed (i.e., this group follows the taxonomy of Fensome and Williams (2004). Sporomorph taxonomy follows Stover and Partridge (1973); Macphail et al. (1994); Raine et al. (2011).

### 10 3.1.2 Dinocyst biostratigraphy and palaeogeographic affinity

Regional dinocyst biostratigraphy for the middle Eocene is based on Bijl et al. (2013a). Dinocyst-based environmental interpretation follows Sluijs et al. (2005); Sluijs and Brinkhuis (2009); Frieling and Sluijs (2018). For biogeographic analysis, dinocyst taxa were binned into Antarctic endemics (including bipolar taxa, Southern Ocean endemics and so-called Transantarctic Flora (TF) cf. Wrenn and Beckman (1982)), and non-endemics (including cosmopolitan and mid-/low-latitude taxa) (**Supplementary Data**). We here consider the distinction between these ecogroups as primarily one of temperature affinity, following Bijl et al. (2011). We label taxa without a clear temperature affinity as cosmopolitan, such as those taxa with a distribution that is primarily controlled by other parameters like salinity (e.g., *Senegalinium* cpx.) or nutrient availability (e.g., protoperidinioids). We therefore supplement and update the biogeographical groupings of Bijl et al. (2011) and (2013b) with recent empirical information on ecological affinities of Paleogene dinocysts (Frieling and Sluijs, 2018) (**Supplementary Data**). The mid-/low-latitude ecogroup is composed of taxa that prevail at lower latitudes and higher temperatures, either empirically based (e.g., Frieling and Sluijs, 2018), or with expanded mid-/low-latitude stratigraphic ranges relative to their high-latitude range. Specifically, all wetzellioids and goniodomids are grouped into the mid-/low-latitude ecogroup based on their empirically derived affinity with high temperatures (Frieling and Sluijs, 2018). Southern Ocean endemic taxa are those that are only known from the Southern Ocean, whereas bipolar taxa are those that occur in both the northern and southern high latitudes.

Taxa with unknown biogeographic affinities were excluded from biogeographical analysis. For instance, a large fraction of *Deflandrea* specimens that lost their outer bodies could not be identified to the species level. As some *Deflandrea* species are endemic to the Southern ocean, while others are cosmopolitan, we have excluded these specimens (and other taxa with unknown affinity) from biogeographic analysis. We note that a different choice was made for the middle Eocene dinocyst assemblages from Site 1172, where only the *Deflandrea* species *D. antarctica* is present; consequently, *Deflandrea* inner bodies were counted as *D. antarctica* (Bijl et al., 2011). Notably, endemic and cosmopolitan dinocysts during the MECO at Sites 1170 and 1172 largely consist of two species belonging to the genus *Enneadocysta*, i.e., the cosmopolitan species



*Enneadocysta multicornuta* and the Southern Ocean endemic *Enneadocysta dictyostila*. While both species are morphologically similar, they can be distinguished by their tabulation patterns and the morphology of the distal ends of the processes (Fensome et al., 2006). The species morphology has been crosschecked with the original Site 1172 material and dinocyst counts to validate consistency in species determination. The above biogeographical affinity of dinocysts, in particular the relative abundance of endemic *vs.* non-endemic dinocyst taxa, is used here to distinguish the relative influence of the Antarctic-derived TC *vs.* the lower-latitude-derived EAC and PLC.

### 3.2 Organic geochemistry

To quantify SST changes, 52 samples from ODP Hole 1170D and one sample from the Latrobe-1 core were processed for TEX<sub>86</sub> palaeothermometry based on isoprenoid glycerol dialkyl glycerol tetraether (GDGT) membrane lipids of marine archaea (Schouten et al., 2002). The GDGTs were extracted from freeze-dried, powdered samples (~8–10 g dry weight) with dichloromethane (DCM):methanol (MeOH) (9:1, v/v) using a Dionex accelerated solvent extractor (ASE) 350, at a temperature of 100°C and a pressure of  $7.6 \times 10^6$  Pa. Lipid extracts were subsequently separated by Al<sub>2</sub>O<sub>3</sub> column chromatography into 4 fractions, using hexane:dichloromethane (DCM) (9:1, v/v), ethyl acetate (100%), DCM:MeOH (95:5, v/v) and DCM:MeOH (1:1, v/v). For quantification purposes, 9.9 ng of a C<sub>46</sub> GDGT internal standard (*m/z* 744) was added to the DCM:MeOH (95:5, v/v) fraction after this. This fraction, containing the GDGTs, was subsequently dissolved in hexane:isopropanol (99:1, v/v) to a concentration of ~3 mg/mL, passed through a 0.45 µm polytetrafluoroethylene (PTFE) filter and analysed using ultra-high performance liquid chromatography-mass spectrometry (UHPLC-MS) following (Hopmans et al., 2016). We note that the published TEX<sub>86</sub> records from Site 1172 and the Hampden Section were generated using high performance liquid chromatography-mass spectrometry (HPLC-MS) after (Schouten et al., 2007), but differences in TEX<sub>86</sub> values between the two methods have been shown to be negligible (Hopmans et al., 2016). Samples with very low concentrations (i.e., peak area < 3000 mV and/or peak height < 3x background signal) of any GDGT included in TEX<sub>86</sub> were excluded from analysis. Based on relative abundances of GDGTs, the TEX<sub>86</sub> and Branched versus Isoprenoid Tetraether (BIT) index values were calculated following Schouten et al. (2002) and Hopmans et al. (2004), respectively. The BIT index is used as an indicator for the relative contribution of terrestrially-derived organic material to the marine realm, where a high BIT indicates a relatively large contribution of terrestrial GDGTs, whereas a low BIT indicates dominance of marine-produced GDGTs. BIT index values >0.3 imply TEX<sub>86</sub> might not correctly reflect SST due to contamination by a terrestrial-derived signal (Weijers et al., 2006). Next to this, several other ratios were calculated to evaluate GDGT sourcing and thus the reliability of TEX<sub>86</sub>-based SST estimates. In short, the Methane Index (MI) (Zhang et al., 2011) and GDGT-2/crenarchaeol (Weijers et al., 2011), GDGT-0/crenarchaeol (Blaga et al., 2009), and GDGT-2/GDGT-3 (Taylor et al., 2013) indices are calculated to investigate potential contributions by methanotrophic, methanogenic, and deep-dwelling GDGT producers to the GDGT pool in the sediments. The analytical precision for TEX<sub>86</sub> is ±0.3°C based on long-term analysis of in-house standards. TEX<sub>86</sub>-to-SST calibrations include those based on mesocosm experiments and core-top datasets. We prefer the latter for paleoreconstructions, as these integrate ecological, water-column and diagenetic effects that are not





incorporated in mesocosm experiments. Since our measured  $\text{TEX}_{86}$  values are within the range of the modern core-top dataset ( $\pm 0.73$ ), no extrapolation of the modern  $\text{TEX}_{86}$ -to-SST relationship is necessary, and differences between linearly and exponentially fitted calibrations are small (see for example Extended Data Figure 2 in Cramwinckel et al. (2018)). Here we calculate SST from  $\text{TEX}_{86}$  values using both the exponential  $\text{TEX}_{86}^{\text{H}}$  calibration of Kim et al. (2010) and the linear calibration of O'Brien et al. (2017) (Supplementary Data). Since the resulting values are highly similar, we present only the values from a single calibration, the  $\text{TEX}_{86}^{\text{H}}$  calibration, in our figures. We note that however, the interest of this study primarily lies in comparing spatial differences in SST and not absolute temperature values.

### 3.3 Statistical analyses

To assess the main patterns within the changing dinocyst assemblages at the studied sites, unconstrained ordination was applied. Both Nonmetric MultiDimensional Scaling (NMDS) and Detrended Correspondence Analysis (DCA) were performed, using the R Package Vegan (Oksanen et al., 2015). Whereas DCA assumes a unimodal species response to the environment, NMDS is a distance-based method that does not assume any relationship, which can be considered more neutral because it introduces less assumptions (Prentice, 1977). For NMDS, the Bray-Curtis measure was used as an appropriate dissimilarity index for (paleo-) ecological community data (e.g., Faith et al., 1987), and recommendations by Clarke (1993) were followed to set the number (two or three) of dimensions used in the ordination. Unconstrained ordination was performed on the full dinocyst assemblages from Site 1170 and Hampden Beach (this study) and Site 1172 (Bijl et al., 2010, 2011, 2013a). The number of Latrobe-1 samples is too small for ordination purposes. Furthermore, unconstrained ordination was applied to the combined dinocyst assemblages of Site 1170, Site 1172, Otway Basin and Hampden Beach.

To investigate whether dinocyst assemblage change at Site 1170 correlates with environmental change, constrained ordination using Canonical Correspondence Analysis (CCA) was performed with the R Package Vegan. We assess different sets of environmental proxy data, including SST (based on  $\text{TEX}_{86}$ ; this study), input of terrestrial material (BIT; this study), shipboard-generated clay contents from smear slide analysis, uranium contents (instead of very sparsely sampled total organic carbon (TOC)), magnetic susceptibility, and colour reflectance data (Mascle et al., 1996). Higher-resolution environmental data were interpolated to the sampling resolution used here for palynology. Like DCA, CCA assumes a unimodal species response to the input environmental variables.

## 4 Results

### 4.1 Site 1170

#### 4.1.1 Palynology

Middle Eocene palynomorphs at Site 1170 are generally well preserved and assemblages are dominated (>95%) by marine forms, mainly dinocysts. Terrestrial palynomorphs occur consistently, but in low relative abundances (<2% of



palynomorphs). The presence of *Impagidinium* spp. in all samples indicates an open marine setting (Dale, 1996), suggesting that palynomorphs characteristic for inshore environments have been transported off-shelf, possibly from the north. Absolute concentrations of dinocysts are extremely high, averaging ~175,000 dinocysts per gram of dry sediment over the studied section, with maxima of over 400,000 cysts per gram. The dinocyst assemblages are generally of low diversity and consist of three dominant groups that typically comprise over 90% of the total dinocysts. These groups are: *Enneadocysta dictyostila*, *Deflandrea* spp. and spiny peridinioids *sensu* Sluijs et al. (2009). High abundances of *Enneadocysta* spp. and peridinioid dinocysts in combination with low diversity indicate a somewhat restricted, eutrophic assemblage with possible low-salinity influences. Endemic taxa dominate the record, typically accounting for more than half of the assemblage (**Figure 3**). The most dominant endemic species is *E. dictyostila*, particularly from 570–690 mbsf. Endemic *Vozzhennikovia apertura* also has a high average relative abundance (~20%). Other, rarer endemics include *Arachnodinium antarcticum*, *Deflandrea antarctica*, *Enneadocysta brevistila*, *Octodinium askiniae*, *Spinidinium macmurdoense*, *S. schellenbergii*, and *Vozzhennikovia netrona*. Cosmopolitan and mid-/low-latitude dinocyst species on average make up about 10% of the assemblage, consisting *a.o.* of *Cerebrocysta* spp., *Cordosphaeridium* spp., *Enneadocysta multicornuta*, *Eocladopyxis peniculata*, *Operculodinium centrocarpum*, and *Thalassiphora pelagica*.

15

#### 4.1.2 Organic geochemistry and sea-surface temperatures

Out of 52 samples from Hole 1170D, five were disregarded for TEX<sub>86</sub> analysis due to low GDGT concentrations, particularly in the lower part of the section. The remaining 47 samples have isoprenoid GDGT concentrations of on average 18 ± 10 ng per g sediment. BIT index values (Hopmans et al., 2004) are consistently below 0.25, indicating a dominant marine source of the isoprenoid GDGTs at this site (Weijers et al., 2006). Furthermore, MI values (Zhang et al., 2011) and GDGT-2/Cren ratios (Weijers et al., 2011) are below 0.3 and 0.2, respectively, indicating no substantial GDGT contributions by methanotrophic archaea. Finally, GDGT-0/Cren ratios (Blaga et al., 2009) are never above 1.2, indicating normal marine conditions, without substantial contributions by methanogenic archaea. Based on the TEX<sub>86</sub><sup>H</sup> calibration, TEX<sub>86</sub>-derived SSTs are mostly between 20–28°C, similar to time-equivalent temperatures at the East Tasman Plateau (Bijl et al., 2010) (**Figure 3**). Maximum temperatures of ~28°C are reached around 670 mbsf, and temperatures decline gradually towards the top of the studied section. Large temperature variability of several degrees between consecutive samples is recorded particularly in the interval from 600 to 550 mbsf (**Figure 3**).

25

#### 4.1.3 Biochronostratigraphic framework

*Selenopemphix* spp. and *Impagidinium parvireticulatum* are present throughout the investigated samples from Site 1170. Their regional first occurrences are at 48.6 Ma and 44.0 Ma, respectively (Bijl et al., 2013a), implying that all studied sediments are younger than 44 Ma. The single occurrence of *Lophocysta* spp. at 569 mbsf provides a narrow age range around the MECO for this part of the investigated core, from 41.39 to 39.66 Ma. We consider the recorded TEX<sub>86</sub>-based temperature maximum at ~670 mbsf to reflect the peak of the MECO and the following cooling trend to represent

30



subsequent surface ocean cooling. This interpretation implies (very) high sedimentation rates in the order of 10s of centimetres per thousand years, consistent with the middle Eocene locality of Site 1170 in a depocenter on the northeast-southwest rifting South Tasman Rise (**Figure 2b-c**). More tentatively, MECO cooling seems to have occurred in two distinct steps in upper ocean temperature records from the Southern Ocean (Bijl et al., 2010; Bohaty et al., 2009) and the equatorial Atlantic ocean (Cramwinckel et al., 2018). The short warming feature in between these cooling steps might be recorded and expanded at 570–600 mbsf at Site 1170 (**Figure 3**). While these constraints are valuable in delimiting our study interval to the MECO, stratigraphic correlation based on temperature proxies is precarious and the lack of precise and consistent age-depth tie-points impedes the construction of a solid age–depth model. We therefore conservatively report our results in the depth domain.

## 4.2 Otway Basin

### 4.2.1 Marine palynology

The palynomorph assemblages from the Latrobe-1 borehole consist predominantly of sporomorphs. Absolute concentrations of dinocysts are in the order of 100–1,000 cysts per gram of dry sediment, while sporomorphs total 2,000–5,000 grains per gram of dry sediment. Although the relative abundance of marine palynomorphs is low, counts of ~50–100 identified dinocysts were possible and some additional prasinophytes and acritarchs were encountered. The *Spiniferites* complex is dominant (averaging ~40 %), and *Enneadocysta* spp. (mostly consisting of *E. multicornuta*) are common (averaging ~20 %). Other minor constituents include *Cleistosphaeridium* spp., *Cordosphaeridium* spp., *Deflandrea* spp., *Elytrocysta* spp., *Hystrichosphaeridium* spp., and *Phthanoperidinium* spp. Notably, the dinocyst assemblages do not contain Antarctic endemic taxa; instead, they are composed solely of cosmopolitan and low-/mid-latitude taxa. Combined, the marine palynology indicates a proximal marine setting.

### 4.2.2 Terrestrial palynology

The middle Eocene sporomorph assemblage from the Latrobe-1 borehole consists of abundant gymnosperm (30–50 %) and angiosperm (30–50 %) pollen, with pteridophyte spores as a minor component of the assemblage (10–15 %). Saccate pollen are mainly represented by *Podocarpidites* spp. (*Podocarpus*), *Lygistepollenites* (*Dacrydium*) and *Phyllocladites* spp. (*Lagarostrobus*); other gymnosperms are Araucariaceae (10–20 %), which consist mainly of *Dilwynites* spp. (*Agathis/Wollemlia*) and, to a lesser extent, of *Araucariacites* spp. (*Araucaria*). Angiosperm pollen are dominated by *Myricipites* spp. (Casuarinaceae; *Gymnostoma*), *Nothofagidites* (including *Nothofagus* sg. *Brassospora*) and *Malvacipollis* spp. (*Austrobuxus/Dissilaria*), with *Proteacidites* spp. and *Rhoipites* spp. as minor elements. Pteridophyte spores are mainly represented by *Cyathidites* spp. and *Laevigatisporites* spp. Furthermore, minor occurrences of *Cycadopites* spp. (Cycadophyta), *Arecipites* spp. (Arecaceae), and *Santalumidites* spp. (*Santalum*) are recorded. Within the sporomorph assemblages, there is a slight dominance shift between the major pollen groups towards the top of the interval: the percentages of saccate pollen increase from ~15–20 % to ~40 % upsection, while angiosperms decrease from ~40–60 % to



~25 %. Simultaneously, the percentages of *Dilwynites* spp. decrease, and *Proteacidites* spp. and *Rhoipites* spp. become relatively less abundant towards the top. In contrast, the percentages of Pteridophytes remain largely constant.

#### 4.2.3 Organic geochemistry

- 5 The analysed sample from the Latrobe-1 borehole contains predominantly terrestrial-derived branched GDGTs, resulting in a BIT index of 0.79, making the sample unsuitable for TEX<sub>86</sub> analysis.

#### 4.2.4 Stratigraphy

- Our new palynological data further constrain the position of the early-middle Eocene hiatus that was recognised in the  
10 Latrobe-1 borehole between 67.35 and 97.84 mbs (Frieling et al., 2018a) to a depth between 78.98 and 70.32 mbs. The hiatus therefore likely corresponds to the transition between the Dilwyn Formation (Wangerrip Group) and the Narraturk Marl (Nirranda Group) at ~70.5 mbs. Dinocyst species with biostratigraphic value in strata above the unconformity include *Phthanoperidinium comatum* (FO 45.70 ± 0.20 Ma) and *Phthanoperidinium stockmansii* (FO 57.20 ± 0.20 Ma), *Achilleodinium biformoides* (recorded as single sample in ODP Site 1171 South Pacific Dinocyst Zone (SPDZ) 13), and  
15 *Dracodinium rhomboideum* (FO 40.00 ± 0.10 Ma) (Bijl et al., 2013a). The interval from 61.46 to 70.32 mbs in the Latrobe-1 borehole is therefore assigned to SPDZ13 (40.0–35.95 Ma), close to the MECO, based on the regional dinocyst zonation of Bijl et al. (2013a). Moreover, the findings of *Dracodinium rhomboideum* in samples at 63.82 and 67.35 mbs designate these depths (the middle two of the four studied middle Eocene samples) to the MECO interval.

### 4.3 Hampden Beach

#### 20 4.3.1 Palynology

- Middle Eocene palynological assemblages at Hampden Beach are dominated by dinocysts (~65 %), with abundant sporomorphs (~30 %) and some acritarchs and prasinophytes. Sediments yield several thousand dinocysts per gram of dry sediment. The consistent presence of *Impagidinium* spp. (mean: ~7 %) indicates an open-ocean setting. The dinocyst assemblages comprise predominantly cosmopolitan and low-/mid-latitude taxa. Similar to the assemblages from the Latrobe-  
25 1 borehole, the outer neritic *Spiniferites* cpx. is dominant (averaging ~40 %). Other common cosmopolitan and low-/mid-latitude taxa include *Cordosphaeridium fibrospinosum*, *Dapsilidinium* spp., *Elytrocysta brevis*, *Hystrichokolpoma rigaudiae*, *Hystrichosphaeridium tubiferum*, and *Senegalinium* spp. (together averaging ~35 %). Antarctic endemic species occur sparsely (averaging ~6 %) and consist of *Deflandrea antarctica*, *Enneadocysta dictyostila* and *Pyxidinoopsis delicata*. The presence of these dinocyst taxa is in agreement with the age of c. 41.7 Ma as previously assigned to the section (Burgess et  
30 al., 2008).



## 5 Discussion

### 5.1 Surface-ocean circulation in the Southwest Pacific during the MECO

Together, our new dinocyst biogeographic data are consistent with previous interpretations of Tasman Gateway surface-ocean circulation based on plankton biogeography and model simulations (Bijl et al., 2011; Huber et al., 2004; Sijp et al., 2016) (**Figure 1b**). By the middle Eocene, the Antarctic endemic dinocyst assemblage associated with the proto-ACC and TC had become firmly established, while the AAG was primarily influenced by the low-latitude-derived PLC. Records from southern New Zealand yield a predominantly warm EAC signal, with a minor, yet constant influx of Antarctic endemics indicating limited TC influence. Throughout the studied middle Eocene interval, dinocyst assemblages at Site 1170 are dominated by Antarctic-endemic taxa. This implies that the Tasman Gateway was influenced by westward atmospheric and surface-oceanic circulation (i.e., the polar easterlies) around 40 Ma, with the 60° S front thus located to the north of the gateway and the proto-ACC flowing through the Tasman Gateway (**Figure 1b**). This is supported by the similar range of TEX<sub>86</sub> SSTs of 20–24°C within (Site 1170) and east of (Site 1172) the Tasman Gateway (**Figure 3**). In terms of paleolatitude reconstructions, placing Site 1170 within the Tasman Gateway south of 60°S at this time is within the uncertainty limits of both commonly used mantle (e.g., Matthews et al., 2016) and paleomagnetic reference frames (e.g., Torsvik et al., 2012). Notably, however, the incursion of cosmopolitan dinocysts that occurs at the zenith of MECO warmth on the East Tasman Plateau (Site 1172) has no equivalent on the South Tasman Rise (Site 1170) (**Figure 3**). These taxa were thus not transported eastward through the Tasman Gateway from a PLC source. Neither can the presence of cosmopolitan dinocysts at Site 1172 be explained by transport from a warming TC and Ross Sea gyre, as this would have transported a similar dinocyst assemblage to Site 1170. Instead, the source of cosmopolitan species may have been southward extension and/or intensification of the EAC (**Figure 1c**). We suggest that transported cosmopolitan species only became dominant at Site 1172 under conditions of peak MECO warmth. Increased southward reach of transported warmth by the EAC has been suggested before as a mechanism to warm the SWP in the early Eocene (Hines et al., 2017; Hollis et al., 2012), as was recently shown to be plausible based on simulations with the Community Earth System Model 1 using 38 Ma geographic boundary conditions (Baatsen et al., 2018). Additionally, uplift of shallow rises in the Tasman Sea during the Eocene may have reoriented the EAC (Sutherland et al., 2018), which could be a promising scenario for modelling studies to investigate.

### 5.2 Drivers of dinocyst assemblage change in the Tasman Gateway

Unconstrained ordination using a unimodal (DCA) or non-metric (NMDS) model shows that the primary variability in the dinocyst assemblage at Site 1170 is governed by *E. dictyostila* and mimics SST quite closely (**Figure 4a, Supplementary Figure 1**), suggesting abundance of *E. dictyostila* responds to temperature. The first NMDS and DCA axes are virtually identical, with DCA1 accounting for 33 % of the variance in the dataset. Both DCA2 (accounting for 17 %) and MDS2 contrast *D. antarctica* and *T. pelagica* at one end of the axis with *Vozzhennikovia* spp. at the other end. Interestingly, ordination results of the MECO and the surrounding interval at Site 1172 are closely comparable with those of Site 1170



(**Figure 4b**, **Supplementary Figure 1**). At Site 1172, the abundance of *E. dictyostila* also controls the first axis (DCA1 accounting for 42 % of the variance), and the second axis (accounting for 17 %) places *D. antarctica* and *T. pelagica* vs. *Vozzhennikovia* spp. No clear patterns in biogeographic or coastal proximity grouping emerge from the ordination results of Site 1170 and Site 1172. However, unconstrained ordination of the combined dinocyst assemblages from Site 1170, Site 1172, the Otway Basin, and Hampden Beach results in a biogeographic separation on the first axis (DCA1 accounting for 77 % of the variance, DCA2 accounting for 38 %) (**Figure 5**). DCA1 and MDS1 separate the Site 1170 and Site 1172 assemblages from the Otway Basin and Hampden Beach assemblages, as these axes separate endemic (and some cosmopolitan) taxa on the left vs. mid-/low-latitude (and some cosmopolitan) taxa on the right. The second axis further separates Site 1170 from Site 1172.

10

The role of temperature in determining assemblage variability at Site 1170 is further supported by constrained ordination (CCA), in which the first axis has high explanatory power (~67 % of the total accounted variance by the environmental variables), and has TEX<sub>86</sub> as the dominant component (**Figure 4c**; environmental variables as time series in **Supplementary Figure 2**). Therefore, although no peak of low-latitude species characterizes the MECO at Site 1170, the ordination analyses suggest that the dinocyst assemblage as a whole, and in particular *E. dictyostila*, responded to temperature change during MECO.

15

Taken together, these results confirm previous evidence that once a surface-oceanography-tracking plankton community has been established, relative abundance changes within the community correspond closely with changes in SST (cf. Bijl et al., 2011). In the modern ocean, phytoplankton distribution patterns are driven by the interplay of passive transport by surface currents and temperature selection (Hellweger et al., 2016; Thomas et al., 2012). A similar dual selection mechanism seems to have affected the middle Eocene dinocyst assemblages in the region. Regional surface-ocean circulation determined which assemblage was established and where. This spatial pattern (**Figure 5**) could change over tectonic timescales as paleogeography changed (Bijl et al. 2011). Dominance shifts and variability within these assemblages were then driven by superimposed surface-ocean changes (such as in temperature), which typically occur on shorter timescales.

25

### 5.3 Massive middle Eocene dinocyst productivity on the South Tasman Rise

At the South Tasman Rise, MECO sediments are not only characterised by rapid sedimentation rates (in the order of 10s of cms per kyr according to our age models; compare Section 4.1.3), but also by high concentrations of dinocysts (**Figure 6**). High sedimentation rates are readily explained by the location of Site 1170 as a middle Eocene depocenter affected by rifting between Australia and Antarctica and associated subsidence (Exon et al., 2004). However, the extraordinarily high dinocyst concentrations are more difficult to explain. They are 100–1,000 times higher than in the studied strata from the Otway Basin and Hampden Beach. They also stand out when compared to other time intervals and settings where high dinocyst concentrations are expected and found. Specifically, they are about an order of magnitude higher than those typically found

30



in Mediterranean sapropels (e.g., Sangiorgi et al., 2006; van Helmond et al., 2015; Zwiép et al., 2018), Cretaceous Oceanic Anoxic Event 2 shelf sediments (van Helmond et al., 2014) and the Holocene Adélie drift underlying a highly productive polynya system (Hartman et al., 2018). The average dinocyst concentrations at Site 1170 may be converted to average accumulation rates in the order of 10,000–80,000 cysts per cm<sup>2</sup> per yr. This range of fluxes was derived using shipboard measured sediment densities (Exon et al., 2001) and by assuming our SST record represents peak MECO and (partially) subsequent cooling, and assigning this a duration between 50 and 300 kyr, as there is large uncertainty on the duration of MECO recovery (e.g., Bohaty et al., 2009; Bijl et al., 2013a).

The high sedimentation rates and silty claystone facies make it unlikely that high dinocyst content was the result of sediment starvation and/or winnowing, respectively. Furthermore, such conditions would also have facilitated oxidation and degradation of organic-walled palynomorphs, while they are instead well-preserved and abundant. Therefore, these high concentrations seem to represent extreme dinocyst productivity and/or preservation. Enhanced sediment accumulation rate by itself facilitates burial of organic matter, in particular through adsorption of organics to clay minerals (Berner, 2006; Hedges and Keil, 1995), so preservation likely played a role. However, total organic carbon (TOC) contents are not extremely high (mean: ~1 % over the studied interval), the sediment is well bioturbated, and there is no significant correlation between dinocysts/gram and shipboard TOC contents, uranium contents or magnetic susceptibility (**Supplementary Figure 3**), which suggests preservation was not the driving factor leading to high dinocyst concentrations. Rather, surface ocean productivity might have been elevated. The relatively low diversity of the dinocyst assemblages in combination with the high dominance of a single taxon (*Enneadocysta dictyostila* in the MECO interval) suggests a generally eutrophic setting that could have been characterised by seasonal plankton blooms. Notably, in several records from the Paleocene-Eocene Thermal Maximum (Harding et al., 2011; Sluijs et al., 2011; Frieling et al., 2018b), and a record from Oceanic Anoxic Event 2 at Bass River (van Helmond et al., 2014), highest concentrations of dinocysts reach into the 10,000–100,000 cysts per gram sediment, and also correspond to low diversity - high dominance assemblages, suggestive of dinoflagellate blooms. Dinocysts deriving from heterotrophic dinoflagellates are present at Site 1170, but not in high abundance (**Supplementary data**). This suggests that primary production based on dinoflagellate prey species such as diatoms (Jeong, 1999) was not necessarily high during the studied interval. Combined, the above suggests that high surface-ocean dinoflagellate-based productivity in combination with increased production of resting cysts, was the most likely cause of rapid accumulation of dinocysts at Site 1170, with possible secondary roles for sediment transport and organic matter preservation. Indications why conditions in the middle Eocene Tasman Gateway would have been extremely favourable for dinoflagellate or dinocyst production are, however, yet lacking.



#### 5.4 Southeast Australian vegetation during the MECO

The middle Eocene sporomorph assemblages from the Latrobe-1 borehole are generally similar to those identified in previous studies (Macphail et al., 1994; Greenwood et al., 2003; Hill, 2017), but seem to include a larger proportion of meso- and megathermal components. The sporomorph record at Latrobe-1 reveals that the middle Eocene (~MECO) vegetation of coastal southeast Australia consisted of a mosaic of mesothermal rainforest flora. These forests were dominated by warm temperate angiosperms Casuarinaceae (*Gymnostoma*), *Austrobuxus/Dissilaria* and Proteaceae as shrubs and trees, with rare presence of (paratropical) tree palms (Arecaceae) and cycads (Cycadophyta). Overstorey elements included *Nothofagus* sg. *Brassospora* and gymnosperms of the Araucariaceae and Podocarpaceae (*Podocarpus*, *Dacrydium* and *Lagarostrobos*). The low abundance of saccate Podocarpaceae pollen, *i.e.*, pollen with high transport capability that are often overrepresented in pollen assemblages, suggests that these taxa were not a major part of the coastal vegetation in the lower interval. Together with small trees and shrubs, ground ferns (Gleicheniaceae and Osmundaceae) and tree ferns (Cyatheaceae) occupied the understorey in these rainforests. A decrease in mesothermal rainforest elements together with the absence of Arecaceae pollen in the topmost sample suggests a slight cooling towards the top of the interval. Although the MECO marker dinocyst species *Dracodinium rhomboideum* was recorded in two of four studied samples, further stratigraphic constraints are lacking. Future regional pollen studies focussing on the Nirranda group might therefore elucidate whether the relatively warm-loving flora described here was restricted to the MECO interval, or to a broader interval of middle-late Eocene “background” conditions.

#### 5.5 Sea-level rise during the MECO?

In the Otway Basin, basal Nirranda group sediments of middle Eocene age overlie a large unconformity at the top of the Wangerrip group (e.g., Krassay et al., 2004). This Wilson Bluff transgression overlying the top Latrobe unconformity or Lutetian gap (Holdgate et al., 2003) is recognised throughout southeast Australia (McGowran et al., 2004). It has also been correlated to the Khirthar transgression (Jauhri and Agarwal, 2001; McGowran et al., 2004), a major transgression phase recognised in the Indo-Pacific. While there is seismostratigraphic evidence for regional tectonic rifting, normal faulting and subsidence during the Paleocene and early Eocene in southeast Australia (Krassay et al., 2004; Close et al., 2009), it is unknown when exactly the subsidence terminated and renewed. The long duration of the hiatus separating the Wangerrip group from the Nirranda group suggests at least a cessation of subsidence by the end of the early Eocene (51 Ma). The Wilson Bluff transgression indicates that at some point during the middle Eocene accommodation space was created again, which could have been caused by renewed subsidence or a climate-induced eustatic sea-level rise. The resumption of sedimentation accumulation above the top Latrobe unconformity has been previously dated to between 44 and 40 Ma (Holdgate et al., 2003; McGowran et al., 2004). Based on our new dinocyst-based age constraints, it is likely that the sediments overlying the Wangerrip group are close to the MECO in age, suggestive of a causal link between the Wilson Bluff transgression and MECO warming. Indeed, a global sea-level rise during the MECO (Dawber et al., 2011) could have





facilitated the shift from an erosional to a depositional sedimentary regime. A similar timing of renewed sedimentation occurred in the Schöningen section in the North German Basin, where the transgressive, fully marine Annenberg formation unconformably overlies the Lutetian coal-bearing Helmstedt formation (Riegel et al., 2012). The Annenberg formation has been assigned an age around the MECO (Gürs, 2005), possibly ~41 Ma (Brandes et al., 2012). Based on a compilation of  
5 New Jersey coastal plain sections, a highstand (sequence E8) is also interpreted at ~41–40 Ma (Browning et al., 2008).

Sea-level rise during the MECO could have accommodated increased burial of biogenic carbonate on continental shelves, explaining a reduction in carbonate burial in the deep sea (Sluijs et al., 2013), along with a diminished silicate weathering feedback (Van der Ploeg et al., 2018). However, it should be noted that the above inferences regarding global sea-level rise  
10 during the MECO are very tentative. A dating accuracy of  $\leq 100,000$  years would be required for these transgressive surfaces to indicate their relationship to MECO warming, which is presently not available. It is therefore crucial to improve these constraints in order to assess the potential influence of sea-level change on the carbon cycle during the MECO.

## 6 Conclusions

15 Comparison of plankton and sea-surface temperature patterns during the MECO at the South Tasman Rise indicate that while dinocyst assemblages responded to surface-water warming, they do not yield evidence for increased eastward surface-water throughflow through the Tasman Gateway during peak MECO. This implies that the acme in cosmopolitan taxa at the East Tasman Plateau was likely the result of a southward extension of the EAC during the zenith of MECO warmth, and shows how profoundly surface-ocean currents can respond to external climate forcing in these regions of the Southern  
20 Ocean. This conclusion however, is difficult to reconcile with the strong similarities in paleotemperatures between the STR and ETP. The distinctive middle Eocene setting of Site 1170 is characterized by extremely high sedimentation rates of 10s of cms per kyr and a massive production (and/or transport and preservation) of dinocysts. While high sedimentation rates can be reconciled with the graben-like setting of the locality, the large amounts of dinocysts remain enigmatic. Terrestrial palynomorph assemblages suggest a warm temperate rainforest with some paratropical elements that grew along the  
25 southeast Australian margin during the MECO. Finally, we suggest that the southeast Australian Wilson Bluff Transgression may be related to global sea-level rise during the MECO, but improvement of the available age constraints is necessary to establish a possible causal link.

## Acknowledgements

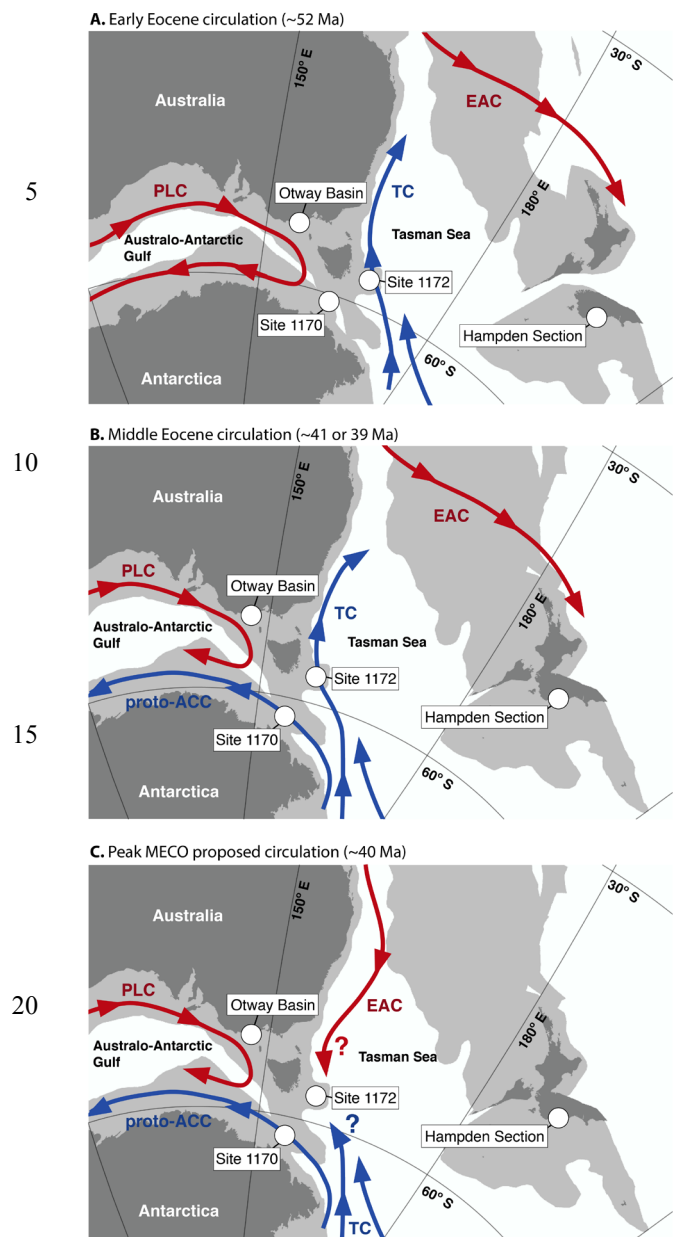
30 This research used samples and data provided by the International Ocean Discovery Program (IODP) and its predecessors. This work was carried out under the program of the Netherlands Earth System Science Centre (NESSC), financially supported by the Dutch Ministry of Education, Culture and Science. This study was made possible by the Netherlands Organisation for Scientific Research (NWO) grant number 834.11.006, which enabled the purchase of the UHPLC-MS



system used for GDGT analyses. Funding was provided by the Australian IODP office and the ARC Basins Genesis Hub (IH130200012) to SJG. We thank Natasja Welters, Jan van Tongeren and Arnold van Dijk (Utrecht University Geolab) for analytical support.



## Main figures

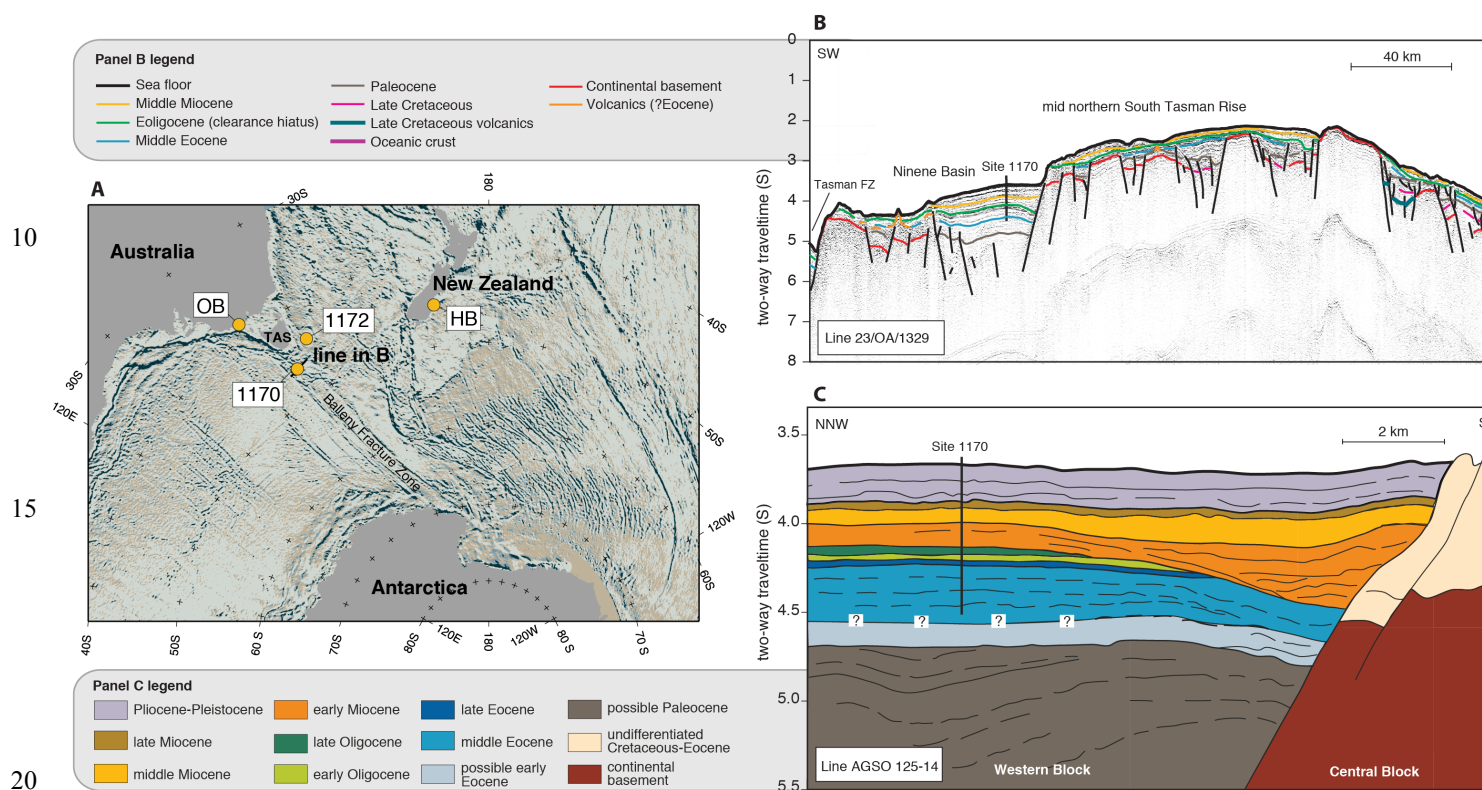


25 **Figure 1. Generalised Eocene surface ocean circulation patterns in the southwest Pacific Ocean.** (a) Generalised early Eocene (~52 Ma) circulation. (b) Generalised middle Eocene circulation pre-MECO (~41 Ma) and post-MECO (~39 Ma). (c) Generalised peak MECO (~40 Ma) circulation. Maps constructed with GPlates, using Torsvik et al. (2012) paleomagnetic rotation frame and Matthews et al. (2016) continental polygons and coastlines for 52 Ma (a) and 40 Ma (b and c). Currents drawn after reconstructions by Bijl et al. (2011, 2013b, 2013a) and this study. EAC = East-Australian Current; PLC = Proto-Leeuwin Current; TC = Tasman Current; proto-ACC = proto-Antarctic Counter Current.

30



5



10

15

20

25

30

**Figure 2. Tectonic setting of ODP Site 1170 and other studied sites** (a) Present-day bathymetry of the Australo-Antarctic sector of the Southern Ocean, with present-day locations of sites and sections used in this study as yellow circles (ODP Site 1170; ODP Site 1172; OB, Otway Basin; HB, Hampden Beach). NW-SE structural trends mark the direction of rifting between Australia and Antarctica, clearly visible in the (labelled) Balleny Fracture Zone. Seismic profile line 23/OA/1329, as shown in panel b, drawn as thick black line. Seismic profile line AGSO125-14 not drawn due to its small scale. Adapted from Bijl et al. (2013b) and Cande and Stock (2004). (b) Interpreted SW-NE seismic profile (line SO36-58) across the South Tasman Rise, illustrating the Site 1170 location in a graben structure. Profile and interpretation adapted from Hill and Moore (2001). (c) Interpreted NNW-SSE seismic profile (line AGSO125-14) across the South Tasman Rise, including Site 1170, illustrating laterally thinning seismic layers of interpreted middle Eocene age. Profile and interpretation adapted from Exon et al. (2001).

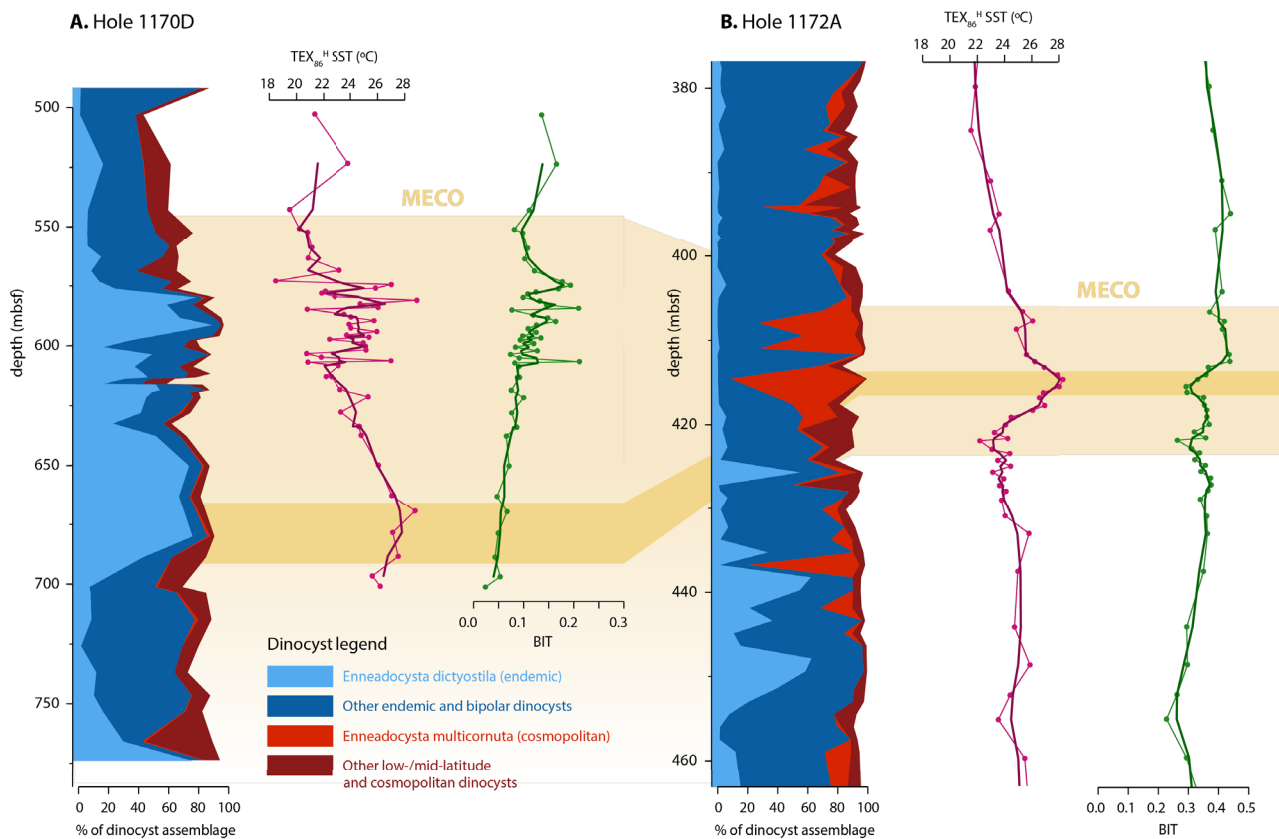


**Figure 3. Dinocyst and temperature data from ODP Site 1170 and Site 1172. (a)** Left: cumulative silhouette plot of relative abundances of selected dinocyst biogeographic groups at Site 1170. Middle: TEX<sub>86</sub><sup>H</sup>-based SST (in degrees celsius) in pink, with 5 point moving average in red. Right: BIT in green, with 5 point moving average in dark green. Plotted against depth in metres below seafloor on the vertical axis. **(b)** Same as a, but for Site 1172. Data from (Bijl et al., 2010, 2011).

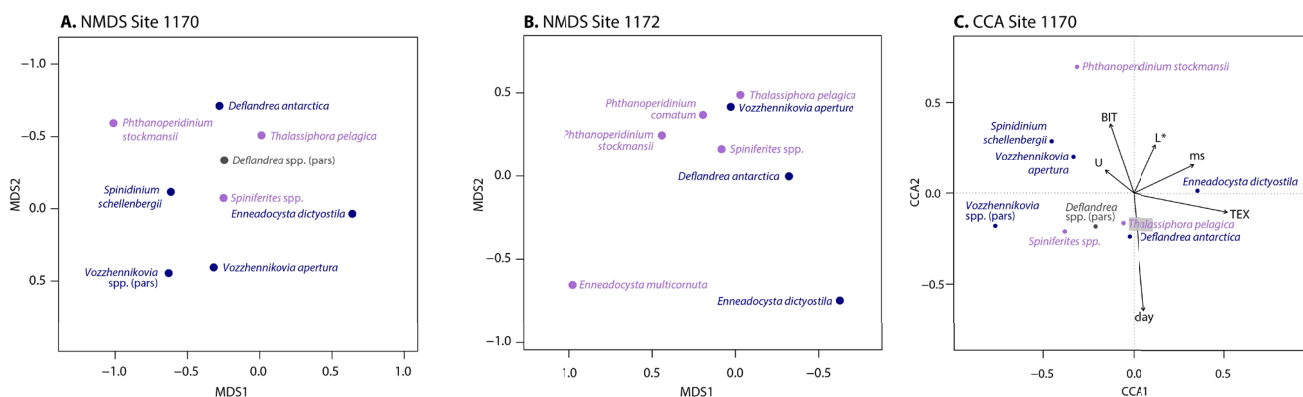


**Figure 4. Ordination results.** (a) Nonmetric multidimensional scaling ordination diagram for the dinocyst assemblage data of Site 1170. Species scores as circles, colour-coded by biogeographic affinity (purple, cosmopolitan; blue, endemic; grey, not assigned). (b) Nonmetric multidimensional scaling ordination diagram for the dinocyst assemblage data of Site 1172. Species colour-coding as in panel a. (c) Canonical correspondence analysis ordination diagram for the dinocyst assemblage data of Site 1170. Species colour-coding as in panel a. Abbreviations are as follows: BIT, BIT index; clay, clay fraction (%); L\*, CIELAB lightness variable; ms, magnetic susceptibility; TEX, TEX<sub>86</sub>; U, uranium content. Total amount of inertia in species data explained by environmental variables is 34%. For visual clarity, only the most abundant taxa (taxa that occur in >10% of the samples, have a mean relative abundance >1%, and have a maximum relative abundance of >5%) are shown in these plots. Ordination plots showing all taxa are provided as Supplementary Figure 1.

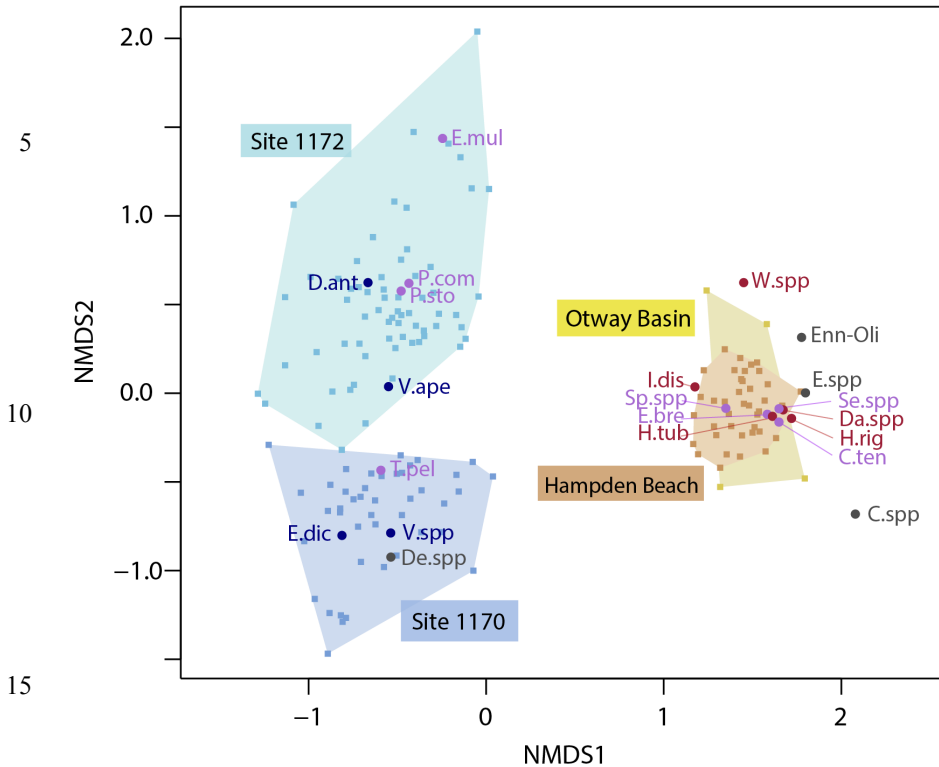


**Figure 5. Nonmetric multidimensional scaling ordination diagram for the combined dinofossil assemblage data of Site 1170, Site 1172, Hampden Beach and Otway Basin.** Species scores as circles, colour-coded by biogeographic affinity (red, mid-/low-latitude; purple, cosmopolitan; blue, endemic; grey, not assigned). Samples scores as squares, colour-coded by location (light blue, Site 1170; dark blue, Site 1172; orange, Hampden Beach; yellow, Otway Basin), with shading connecting same-location samples. Abbreviations are as follows: C.spp, *Corrudinium* spp. (pars); C.ten, *Cribooperidinium tenuitubulatum*; Da.spp, *Dapsilidinium* spp.; D.ant, *Deflandrea antarctica*; De.spp, *Deflandrea* spp.; E.bre, *Elytrocysta brevis*; E.dic, *Enneadocysta dictyostila*; E.mul, *Enneadocysta multicornuta*; Enn-Oli, *Enneadocysta-Oligosphaeridium* intermediate; E.spp, *Enneadocysta* spp. (pars); H.rig, *Hystrichokolpoma rigaudiae*; H.tub, *Hystrichosphaeridium tubiferum*; I.dis, *Impagidinium dispersitum*; P.com, *Phthanoperidinium comatum*; P.sto, *Phthanoperidinium stockmansii*; Se.spp, *Senegalinium* spp. (pars); Sp.spp, *Spiniferites* spp. (pars); T.pel, *Thalassiphora pelagica*; V.ape, *Vozzhennikovia apertura*; V.spp, *Vozzhennikovia* spp. (pars); W.spp, Wetzellioids.

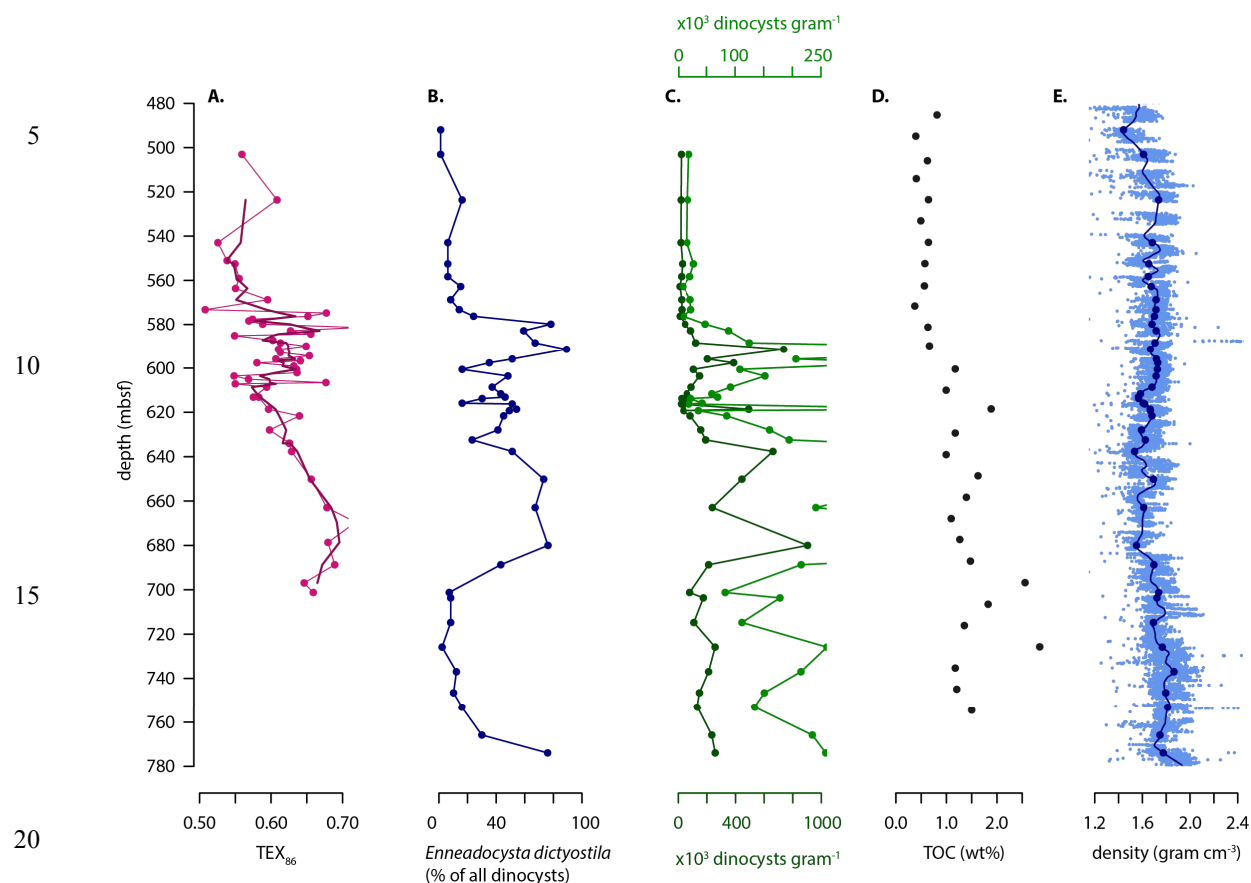


**Figure 6. Selected proxy records over the MECO interval of Site 1170, plotted against depth in metres below sea level. (a)**  $TEX_{86}$  (pink dots and line), with three-point moving average (purple lines). **(b)** Relative abundance of *Enneadocysta dictyostila* (percentage of total dinocyst assemblage; dark blue dots and line). **(c)** Dinoflagellate cyst content (cysts per gram of dry sediment; two different scales shown for visual clarity in dark green and light green). **(d)** Total organic carbon (weight percentage; black dots) (from Exon et al., 2001). **(e)** GRA sediment density in (gram per cubic centimetre; light blue dots original data; dark blue line LOESS fit; dark blue dots interpolated LOESS fit to depth of dinocyst samples) (from Exon et al., 2001).

25  
30





## References

- Abele, C.: Early Eocene Burrungule Member (Wangerrip Group, Gambier Embayment) and middle Eocene Sturgess Point Member (Nirrandra Group, Port Campbell Embayment) in the Otway Basin, southeastern Australia, Geological Survey of Victoria Unpublished Report, (1994/12), 1994.
- 5 Anagnostou, E., John, E. H., Edgar, K. M., Foster, G. L., Ridgwell, A., Inglis, G. N., Pancost, R. D., Lunt, D. J. and Pearson, P. N.: Changing atmospheric CO<sub>2</sub> concentration was the primary driver of early Cenozoic climate, *Nature*, 533(7603), 380–384, doi:10.1038/nature17423, 2016.
- Archer, V.: Palynology of the Victorian Mines Department Latrobe 1 Bore, Otway Basin, Victoria, 1977.
- Baatsen, M., Heydt, A. S. von der, Huber, M., Kliphuis, M. A., Bijl, P. K., Sluijs, A. and Dijkstra, H. A.: Equilibrium state and sensitivity of the simulated middle-to-late Eocene climate, *Climate of the Past Discussions*, 1–49, doi:<https://doi.org/10.5194/cp-2018-43>, 2018.
- 10 Baatsen, M., Heydt, A. S. von der, Huber, M., Kliphuis, M. A., Bijl, P. K., Sluijs, A. and Dijkstra, H. A.: Equilibrium state and sensitivity of the simulated middle-to-late Eocene climate, *Climate of the Past Discussions*, 1–49, doi:<https://doi.org/10.5194/cp-2018-43>, 2018.
- Berner, R. A.: Comment: Mesozoic Atmospheric Oxygen (Comment on “MAGic: A phanerozoic model for the geochemical cycling of major rock-forming components” by Rolf S. Arvidson, Fred T. Mackenzie and Michael Guidry, *American Journal of Science*, v. 306, p. 135–190.), *Am J Sci*, 306(9), 769–771, 2006.
- 15 Bijl, P. K., Schouten, S., Sluijs, A., Reichart, G.-J., Zachos, J. C. and Brinkhuis, H.: Early Palaeogene temperature evolution of the southwest Pacific Ocean, *Nature*, 461(7265), 776–779, doi:10.1038/nature08399, 2009.
- Bijl, P. K., Houben, A. J. P., Schouten, S., Bohaty, S. M., Sluijs, A., Reichart, G.-J., Damsté, J. S. S. and Brinkhuis, H.: Transient Middle Eocene Atmospheric CO<sub>2</sub> and Temperature Variations, *Science*, 330(6005), 819–821, doi:10.1126/science.1193654, 2010.
- 20 Bijl, P. K., Pross, J., Warnaar, J., Stickley, C. E., Huber, M., Guerstein, R., Houben, A. J. P., Sluijs, A., Visscher, H. and Brinkhuis, H.: Environmental forcings of Paleogene Southern Ocean dinoflagellate biogeography, *Paleoceanography*, 26(1), PA1202, doi:10.1029/2009PA001905, 2011.
- Bijl, P. K., Sluijs, A. and Brinkhuis, H.: A magneto- and chemostratigraphically calibrated dinoflagellate cyst zonation of the early Palaeogene South Pacific Ocean, *Earth-Science Reviews*, 124, 1–31, doi:10.1016/j.earscirev.2013.04.010, 2013a.
- 25 Bijl, P. K., Bendle, J. A. P., Bohaty, S. M., Pross, J., Schouten, S., Tauxe, L., Stickley, C. E., McKay, R. M., Röhl, U., Olney, M., Sluijs, A., Escutia, C., Brinkhuis, H., Klaus, A., Fehr, A., Williams, T., Carr, S. A., Dunbar, R. B., González, J. J., Hayden, T. G., Iwai, M., Jimenez-Espejo, F. J., Katsuki, K., Kong, G. S., Nakai, M., Passchier, S., Pekar, S. F., Riesselman, C., Sakai, T., Shrivastava, P. K., Sugisaki, S., Tuo, S., Flierdt, T. van de, Welsh, K. and Yamane, M.: Eocene cooling linked to early flow across the Tasmanian Gateway, *PNAS*, 110(24), 9645–9650, doi:10.1073/pnas.1220872110, 2013b.
- 30 Bijl, P. K., Brinkhuis, H., Egger, L. M., Eldrett, J. S., Frieling, J., Grothe, A., Houben, A. J. P., Pross, J., Śliwińska, K. K. and Sluijs, A.: Comment on ‘Wetzeliella and its allies – the “hole” story: a taxonomic revision of the Paleogene dinoflagellate subfamily Wetzelielloideae’ by Williams et al. (2015), *Palynology*, 6122 (January 2017), 1–7, doi:10.1080/01916122.2016.1235056, 2016.
- 35 Blaga, C. I., Reichart, G.-J., Heiri, O. and Damsté, J. S. S.: Tetraether membrane lipid distributions in water-column particulate matter and sediments: a study of 47 European lakes along a north–south transect, *J Paleolimnol*, 41(3), 523–540, doi:10.1007/s10933-008-9242-2, 2009.



- Bohaty, S. M. and Zachos, J. C.: Significant Southern Ocean warming event in the late middle Eocene, *Geology*, 31(11), 1017–1020, doi:10.1130/G19800.1, 2003.
- Bohaty, S. M., Zachos, J. C., Florindo, F. and Delaney, M. L.: Coupled greenhouse warming and deep-sea acidification in the middle Eocene, *Paleoceanography*, 24(2), PA2207, doi:10.1029/2008PA001676, 2009.
- 5 Boscolo-Galazzo, F., Thomas, E., Pagani, M., Warren, C., Luciani, V. and Giusberti, L.: The middle Eocene climatic optimum (MECO): A multiproxy record of paleoceanographic changes in the southeast Atlantic (ODP Site 1263, Walvis Ridge), *Paleoceanography*, 29(12), 2014PA002670, doi:10.1002/2014PA002670, 2014.
- Boscolo-Galazzo, F., Thomas, E. and Giusberti, L.: Benthic foraminiferal response to the Middle Eocene Climatic Optimum (MECO) in the South-Eastern Atlantic (ODP Site 1263), *Palaeogeography, Palaeoclimatology, Palaeoecology*, 417, 432–  
10 444, doi:10.1016/j.palaeo.2014.10.004, 2015.
- Brandes, C., Pollok, L., Schmidt, C., Wilde, V. and Winsemann, J.: Basin modelling of a lignite-bearing salt rim syncline: insights into rim syncline evolution and salt diapirism in NW Germany, *Basin Research*, 24(6), 699–716, doi:10.1111/j.1365-2117.2012.00544.x, 2012.
- Browning, J. V., Miller, K. G., Sugarman, P. J., Kominz, M. A., McLaughlin, P. P., Kulpecz, A. A. and Feigenson, M. D.:  
15 100 Myr record of sequences, sedimentary facies and sea level change from Ocean Drilling Program onshore coreholes, US Mid-Atlantic coastal plain, *Basin Research*, 20(2), 227–248, doi:10.1111/j.1365-2117.2008.00360.x, 2008.
- Burgess, C. E., Pearson, P. N., Lear, C. H., Morgans, H. E. G., Handley, L., Pancost, R. D. and Schouten, S.: Middle Eocene climate cyclicity in the southern Pacific: Implications for global ice volume, *Geology*, 36(8), 651–654, doi:10.1130/G24762A.1, 2008.
- 20 Cande, S. C. and Stock, J. M.: Cenozoic Reconstructions of the Australia-New Zealand-South Pacific Sector of Antarctica, in *The Cenozoic Southern Ocean: tectonics, sedimentation, and climate change between Australia and Antarctica*, edited by N. F. Exxon, J. P. Kennett, and M. J. Malone, pp. 5–17, American Geophysical Union, Washington, DC. [online] Available from: <http://resolver.caltech.edu/CaltechAUTHORS:20140425-125510082> (Accessed 8 August 2018), 2004.
- Carpenter, R. J., Jordan, G. J., Macphail, M. K. and Hill, R. S.: Near-tropical Early Eocene terrestrial temperatures at the  
25 Australo-Antarctic margin, western Tasmania, *Geology*, 40(3), 267–270, doi:10.1130/G32584.1, 2012.
- Clarke, K. R.: Non-parametric multivariate analyses of changes in community structure, *Australian Journal of Ecology*, 18(1), 117–143, doi:10.1111/j.1442-9993.1993.tb00438.x, 1993.
- Close, D. I., Watts, A. B. and Stagg, H. M. J.: A marine geophysical study of the Wilkes Land rifted continental margin, *Antarctica, Geophys J Int*, 177(2), 430–450, doi:10.1111/j.1365-246X.2008.04066.x, 2009.
- 30 Contreras, L., Pross, J., Bijl, P. K., Koutsodendris, A., Raine, J. I., van de Schootbrugge, B. and Brinkhuis, H.: Early to Middle Eocene vegetation dynamics at the Wilkes Land Margin (Antarctica), *Review of Palaeobotany and Palynology*, 197, 119–142, doi:10.1016/j.revpalbo.2013.05.009, 2013.
- Contreras, L., Pross, J., Bijl, P. K., O’Hara, R. B., Raine, J. I., Sluijs, A. and Brinkhuis, H.: Southern high-latitude terrestrial climate change during the Palaeocene–Eocene derived from a marine pollen record (ODP Site 1172, East Tasman Plateau),  
35 *Clim. Past*, 10(4), 1401–1420, doi:10.5194/cp-10-1401-2014, 2014.



- Cramwinckel, M. J., Huber, M., Kocken, I. J., Agnini, C., Bijl, P. K., Bohaty, S. M., Frieling, J., Goldner, A., Hilgen, F. J., Kip, E. L., Peterse, F., Ploeg, R. van der, Röhl, U., Schouten, S. and Sluijs, A.: Synchronous tropical and polar temperature evolution in the Eocene, *Nature*, 559(7714), 382–386, doi:10.1038/s41586-018-0272-2, 2018.
- 5 Cramwinckel, M. J., Ploeg, R. van der, Bijl, P. K., Peterse, F., Bohaty, S. M., Röhl, U., Schouten, S., Middelburg, J. J. and Sluijs, A.: Harmful algae and export production collapse in the equatorial Atlantic during the zenith of Middle Eocene Climatic Optimum warmth, *Geology*, doi:10.1130/G45614.1, 2019.
- Dale, B.: Dinoflagellate cyst ecology: modeling and geological applications, in Jansonius, J., McGregor, D.C. (Eds.), *Palynology: Principles and Applications*, pp. 1249–1275, AASP Foundation., 1996.
- 10 Dawber, C. F., Tripathi, A. K., Gale, A. S., MacNiocaill, C. and Hesselbo, S. P.: Glacioeustasy during the middle Eocene? Insights from the stratigraphy of the Hampshire Basin, UK, *Palaeogeography, Palaeoclimatology, Palaeoecology*, 300(1–4), 84–100, doi:10.1016/j.palaeo.2010.12.012, 2011.
- Exon, N. F., Kennett, J. P. and Malone, M. J.: *Proceedings of the Ocean Drilling Program Initial Reports*, Ocean Drilling Program, College Station, TX., 2001.
- 15 Exon, N. F., Kennett, J. P. and Malone, M. J.: *The Cenozoic Southern Ocean: Tectonics, Sedimentation, and Climate Change Between Australia and Antarctica*, Wiley., 2004.
- Faith, D. P., Minchin, P. R. and Belbin, L.: Compositional dissimilarity as a robust measure of ecological distance, *Vegetatio*, 69(1), 57–68, doi:10.1007/BF00038687, 1987.
- Fensome, R. A. and Williams, G. L.: *The Lentin and Williams Index of Fossil Dinoflagellates*, American association of stratigraphic palinologists foundation., 2004.
- 20 Fensome, R. A., Guerstein, G. R. and Williams, G. L.: New insights on the Paleogene dinoflagellate cyst genera *Enneadocysta* and *Licracysta* gen. nov. based on material from offshore eastern Canada and southern Argentina, *Micropaleontology*, 52(5), 385–410, doi:10.2113/gsmicropal.52.5.385, 2006.
- Frieling, J. and Sluijs, A.: Towards quantitative environmental reconstructions from ancient non-analogue microfossil assemblages: Ecological preferences of Paleocene – Eocene dinoflagellates, *Earth-Science Reviews*, 185, 956–973, doi:10.1016/j.earscirev.2018.08.014, 2018.
- 25 Frieling, J., Hurdeman, E. P., Rem, C. C. M., Donders, T. H., Pross, J., Bohaty, S. M., Holdgate, G. R., Gallagher, S. J., McGowran, B. and Bijl, P. K.: Identification of the Paleocene–Eocene boundary in coastal strata in the Otway Basin, Victoria, Australia, *Journal of Micropalaeontology*, 37(1), 317–339, doi:<https://doi.org/10.5194/jm-37-317-2018>, 2018a.
- 30 Frieling, J., Reichart, G.-J., Middelburg, J. J., Röhl, U., Westerhold, T., Bohaty, S. M. and Sluijs, A.: Tropical Atlantic climate and ecosystem regime shifts during the Paleocene–Eocene Thermal Maximum, *Clim. Past*, 14(1), 39–55, doi:10.5194/cp-14-39-2018, 2018b.
- Gallagher, S. J. and Holdgate, G.: The palaeogeographic and palaeoenvironmental evolution of a Palaeogene mixed carbonate–siliciclastic cool-water succession in the Otway Basin, Southeast Australia, *Palaeogeography, Palaeoclimatology, Palaeoecology*, 156(1–2), 19–50, doi:10.1016/S0031-0182(99)00130-3, 2000.
- 35 Gallagher, S. J., Jonasson, K. and Holdgate, G.: Foraminiferal biofacies and palaeoenvironmental evolution of an Oligo-Miocene cool-water carbonate succession in the Otway Basin, southeast Australia, *Journal of Micropalaeontology*, 18(2), 143–168, doi:10.1144/jm.18.2.143, 1999.



- Greenwood, D. R., Moss, P. T., Rowett, A. I., Vadala, A. J. and Keefe, R. L.: Plant communities and climate change in southeastern Australia during the early Paleogene, in *Causes and consequences of globally warm climates in the early Paleogene*, edited by S. L. Wing, P. D. Gingerich, B. Schmitz, and E. Thomas, pp. 365–380, Geological Society of America., 2003.
- 5 Gürs, K.: Das Tertiär Nordwestdeutschlands in der Stratigraphischen Tabelle von Deutschland 2002, [online] Available from: <https://www.ingentaconnect.com/content/schweiz/nis/2005/00000041/f0030001/art00021> (Accessed 22 August 2018), 2005.
- Harding, I. C., Charles, A. J., Marshall, J. E. A., Pälike, H., Roberts, A. P., Wilson, P. A., Jarvis, E., Thorne, R., Morris, E., Moremon, R., Pearce, R. B. and Akbari, S.: Sea-level and salinity fluctuations during the Paleocene–Eocene thermal maximum in Arctic Spitsbergen, *Earth and Planetary Science Letters*, 303(1), 97–107, doi:10.1016/j.epsl.2010.12.043, 2011.
- 10 Hartman, J. D., Bijl, P. K. and Sangiorgi, F.: A review of the ecological affinities of marine organic microfossils from a Holocene record offshore of Adélie Land (East Antarctica), *Journal of Micropalaeontology*, 37(2), 445–497, doi:<https://doi.org/10.5194/jm-37-445-2018>, 2018.
- Harwood, D. M.: Cenozoic diatom biogeography in the southern high latitudes: Inferred biogeographical barriers and progressive endemism, in *Geological Evolution of Antarctica: Proceedings of the Fifth International Symposium on Antarctic Earth Sciences*, edited by M. R. A. Thompson et al., pp. 667–673, Cambridge University Press, Cambridge, U.K., 1991.
- 15 Hedges, J. I. and Keil, R. G.: Sedimentary organic matter preservation: an assessment and speculative synthesis, *Marine Chemistry*, 49(2–3), 81–115, doi:10.1016/0304-4203(95)00008-F, 1995.
- 20 Hellweger, F. L., Sebille, E. van, Calfee, B. C., Chandler, J. W., Zinser, E. R., Swan, B. K. and Fredrick, N. D.: The Role of Ocean Currents in the Temperature Selection of Plankton: Insights from an Individual-Based Model, *PLOS ONE*, 11(12), e0167010, doi:10.1371/journal.pone.0167010, 2016.
- van Helmond, N. A. G. M., Sluijs, A., Reichert, G.-J., Damsté, J. S. S., Slomp, C. P. and Brinkhuis, H.: A perturbed hydrological cycle during Oceanic Anoxic Event 2, *Geology*, 42(2), 123–126, doi:10.1130/G34929.1, 2014.
- 25 van Helmond, N. A. G. M., Hennekam, R., Donders, T. H., Bunnik, F. P. M., de Lange, G. J., Brinkhuis, H. and Sangiorgi, F.: Marine productivity leads organic matter preservation in sapropel S1: palynological evidence from a core east of the Nile River outflow, *Quaternary Science Reviews*, 108(Supplement C), 130–138, doi:10.1016/j.quascirev.2014.11.014, 2015.
- Hill, P. J. and Exon, N. F.: Tectonics and Basin Development of the Offshore Tasmanian Area Incorporating Results from Deep Ocean Drilling, in *The Cenozoic Southern Ocean: tectonics, sedimentation, and climate change between Australia and Antarctica*, edited by N. F. Exon, J. P. Kennett, and M. J. Malone, pp. 19–42, American Geophysical Union, Washington, DC., 2004.
- 30 Hill, P. J. and Moore, A. M. G.: Geological Framework of the South Tasman Rise and East Tasman Plateau, *Geoscience Australia*, 2001.
- Hill, R. S.: *History of the Australian Vegetation: Cretaceous to Recent*, University of Adelaide Press., 2017.
- 35 Hines, B. R., Hollis, C. J., Atkins, C. B., Baker, J. A., Morgans, H. E. G. and Strong, P. C.: Reduction of oceanic temperature gradients in the early Eocene Southwest Pacific Ocean, *Palaeogeography, Palaeoclimatology, Palaeoecology*, 475, 41–54, doi:10.1016/j.palaeo.2017.02.037, 2017.



- Holdgate, G. R., Rodriquez, C., Johnstone, E. M., Wallace, M. W. and Gallagher, S. J.: The Gippsland Basin Top Latrobe unconformity, and its expression in other SE Australian basins, *The APPEA Journal*, 43(1), 149–173, doi:10.1071/aj02007, 2003.
- 5 Hollis, C. J., Handley, L., Crouch, E. M., Morgans, H. E. G., Baker, J. A., Creech, J., Collins, K. S., Gibbs, S. J., Huber, M., Schouten, S., Zachos, J. C. and Pancost, R. D.: Tropical sea temperatures in the high-latitude South Pacific during the Eocene, *Geology*, 37(2), 99–102, doi:10.1130/G25200A.1, 2009.
- 10 Hollis, C. J., Taylor, K. W. R., Handley, L., Pancost, R. D., Huber, M., Creech, J. B., Hines, B. R., Crouch, E. M., Morgans, H. E. G., Crampton, J. S., Gibbs, S., Pearson, P. N. and Zachos, J. C.: Early Paleogene temperature history of the Southwest Pacific Ocean: Reconciling proxies and models, *Earth and Planetary Science Letters*, 349–350, 53–66, doi:10.1016/j.epsl.2012.06.024, 2012.
- Hopmans, E. C., Weijers, J. W. H., Schefuß, E., Herfort, L., Sinninghe Damsté, J. S. and Schouten, S.: A novel proxy for terrestrial organic matter in sediments based on branched and isoprenoid tetraether lipids, *Earth and Planetary Science Letters*, 224(1–2), 107–116, doi:10.1016/j.epsl.2004.05.012, 2004.
- 15 Hopmans, E. C., Schouten, S. and Sinninghe Damsté, J. S.: The effect of improved chromatography on GDGT-based palaeoproxies, *Organic Geochemistry*, 93, 1–6, doi:10.1016/j.orggeochem.2015.12.006, 2016.
- Huber, M. and Caballero, R.: The early Eocene equable climate problem revisited, *Climate of the Past*, 7, 603–633, doi:10.5194/cp-7-603-2011, 2011.
- 20 Huber, M., Brinkhuis, H., Stickley, C. E., Döös, K., Sluijs, A., Warnaar, J., Schellenberg, S. A. and Williams, G. L.: Eocene circulation of the Southern Ocean: Was Antarctica kept warm by subtropical waters?, *Paleoceanography*, 19(4), PA4026, doi:10.1029/2004PA001014, 2004.
- Huck, C. E., Fliedert, T. van de, Bohaty, S. M. and Hammond, S. J.: Antarctic climate, Southern Ocean circulation patterns, and deep water formation during the Eocene, *Paleoceanography*, 32(7), 674–691, doi:10.1002/2017PA003135, 2017.
- 25 Inglis, G. N., Farnsworth, A., Lunt, D., Foster, G. L., Hollis, C. J., Pagani, M., Jardine, P. E., Pearson, P. N., Markwick, P., Galsworthy, A. M. J., Raynham, L., Taylor, K. W. R. and Pancost, R. D.: Descent toward the Icehouse: Eocene sea surface cooling inferred from GDGT distributions, *Paleoceanography*, 30(7), 2014PA002723, doi:10.1002/2014PA002723, 2015.
- Jauhri, A. K. and Agarwal, K. K.: Early Palaeogene in the south Shillong Plateau, NE India: local biostratigraphic signals of global tectonic and oceanic changes, *Palaeogeography, Palaeoclimatology, Palaeoecology*, 168(1), 187–203, doi:10.1016/S0031-0182(00)00255-8, 2001.
- 30 Jeong, H. J.: The Ecological Roles of Heterotrophic Dinoflagellates in Marine Planktonic Community1, *Journal of Eukaryotic Microbiology*, 46(4), 390–396, doi:10.1111/j.1550-7408.1999.tb04618.x, 1999.
- Kennett, J. P., Houtz, R. E., Andrews, P. B., Edwards, A. R., Gostin, V. A., Hajos, M., Hampton, M. A., Jenkins, D. G., Margolis, S. V., Owenshine, A. T. and Perch-Nielsen, K.: Development of the Circum-Antarctic Current, *Science*, 186(4159), 144–147, doi:10.1126/science.186.4159.144, 1974.
- 35 Kim, J.-H., van der Meer, J., Schouten, S., Helmke, P., Willmott, V., Sangiorgi, F., Koç, N., Hopmans, E. C. and Damsté, J. S. S.: New indices and calibrations derived from the distribution of crenarchaeal isoprenoid tetraether lipids: Implications for past sea surface temperature reconstructions, *Geochimica et Cosmochimica Acta*, 74(16), 4639–4654, doi:10.1016/j.gca.2010.05.027, 2010.



- Krassay, A. A., Cathro, D. L. and Ryan, D. J.: A Regional Tectonostratigraphic Framework for the Otway Basin, in Eastern Australasian Basins Symposium II, edited by P. J. Boulton, D. R. Johns, and S. C. Lang, pp. 97–116, Adelaide. [online] Available from: <http://archives.datapages.com/data/petroleum-exploration-society-of-australia/conferences/002/002001/pdfs/97.html> (Accessed 24 September 2018), 2004.
- 5 Lagabrielle, Y., Godd eris, Y., Donnadieu, Y., Malavieille, J. and Suarez, M.: The tectonic history of Drake Passage and its possible impacts on global climate, *Earth and Planetary Science Letters*, 279(3), 197–211, doi:10.1016/j.epsl.2008.12.037, 2009.
- Lazarus, D. B., Hollis, C. J. and Apel, M.: Patterns of Opal and Radiolarian change in the Antarctic Mid-Paleogene: Clues to the Origin of the Southern Ocean, *Micropaleontology*, 54(1), 41–48, 2008.
- 10 Lunt, D. J., Dunkley Jones, T., Heinemann, M., Huber, M., LeGrande, A., Winguth, A., Loptson, C., Marotzke, J., Roberts, C. D., Tindall, J., Valdes, P. and Winguth, C.: A model–data comparison for a multi-model ensemble of early Eocene atmosphere–ocean simulations: EoMIP, *Clim. Past*, 8(5), 1717–1736, doi:10.5194/cp-8-1717-2012, 2012.
- Macphail, M. K., Alley, N. F., Truswell, E. M. and Sluiter, I. R. K.: Early Tertiary vegetation: Evidence from spores and pollen, in *History of the Australian vegetation: Cretaceous to Recent*, edited by R. S. Hill, pp. 189–261, University of Adelaide Press, Adelaide., 1994.
- 15 Mascle, J., Lohmann, G. P., Clift, P. D. and Shipboard Scientific Party: *Proceedings of the Ocean Drilling Program Initial Reports*, College Station, TX (Ocean Drilling Program), 1996.
- Matthews, K. J., Maloney, K. T., Zahirovic, S., Williams, S. E., Seton, M. and M ller, R. D.: Global plate boundary evolution and kinematics since the late Paleozoic, *Global and Planetary Change*, 146, 226–250, doi:10.1016/j.gloplacha.2016.10.002, 2016.
- 20 McGowran, B., Holdgate, G. R., Li, Q. and Gallagher, S. J.: Cenozoic stratigraphic succession in southeastern Australia, *Australian Journal of Earth Sciences*, 51(4), 459–496, doi:10.1111/j.1400-0952.2004.01078.x, 2004.
- Nelson, C. S. and Cooke, P. J.: History of oceanic front development in the New Zealand sector of the Southern Ocean during the Cenozoic—a synthesis, *New Zealand Journal of Geology and Geophysics*, 44(4), 535–553, doi:10.1080/00288306.2001.9514954, 2001.
- 25 O’Brien, C. L., Robinson, S. A., Pancost, R. D., Sinninghe Damst , J. S., Schouten, S., Lunt, D. J., Alsenz, H., Bornemann, A., Bottini, C., Brassell, S. C., Farnsworth, A., Forster, A., Huber, B. T., Inglis, G. N., Jenkyns, H. C., Linnert, C., Littler, K., Markwick, P., McAnena, A., Mutterlose, J., Naafs, B. D. A., P ttmann, W., Sluijs, A., van Helmond, N. A. G. M., Vellekoop, J., Wagner, T. and Wrobel, N. E.: Cretaceous sea-surface temperature evolution: Constraints from TEX86 and planktonic foraminiferal oxygen isotopes, *Earth-Science Reviews*, 172(Supplement C), 224–247, doi:10.1016/j.earscirev.2017.07.012, 2017.
- Oksanen, J., Guillaume Blanchet, F., Kindt, R., Legendre, P., Minchin, P. R., O’Hara, R. B., Simpson, G. L., Solymos, P., Stevens, M. H. H. and Wagner, H.: *vegan: Community Ecology Package*. R package version 2.3-0. [online] Available from: <http://CRAN.R-project.org/package=vegan>, 2015.
- 35 Pascher, K. M., Hollis, C. J., Bohaty, S. M., Cortese, G., McKay, R. M., Seebeck, H., Suzuki, N. and Chiba, K.: Expansion and diversification of high-latitude radiolarian assemblages in the late Eocene linked to a cooling event in the southwest Pacific, *Clim. Past*, 11, 1599–1620, doi:10.5194/cp-11-1599-2015, 2015.



- van der Ploeg, R., Selby, D., Cramwinckel, M. J., Li, Y., Bohaty, S. M., Middelburg, J. J. and Sluijs, A.: Middle Eocene greenhouse warming facilitated by diminished weathering feedback, *Nature Communications*, 9(1), 2877, doi:10.1038/s41467-018-05104-9, 2018.
- Prentice, I. C.: Non-Metric Ordination Methods in Ecology, *Journal of Ecology*, 65(1), 85–94, doi:10.2307/2259064, 1977.
- 5 Pross, J., Contreras, L., Bijl, P. K., Greenwood, D. R., Bohaty, S. M., Schouten, S., Bendle, J. A., Röhl, U., Tauxe, L., Raine, J. I., Huck, C. E., van de Flierdt, T., Jamieson, S. S. R., Stickley, C. E., van de Schootbrugge, B., Escutia, C., Brinkhuis, H. and Scientists, I. O. D. P. E. 318: Persistent near-tropical warmth on the Antarctic continent during the early Eocene epoch, *Nature*, 488(7409), 73–77, doi:10.1038/nature11300, 2012.
- Raine, J. I., Mildenhall, D. C. and Kennedy, E. M.: New Zealand fossil spores and pollen: an illustrated catalogue. 4th edition., GNS Science miscellaneous series no. 4 [online] Available from: <http://data.gns.cri.nz/sporepollen/index.htm>, 2011.
- 10 Riegel, W., Wilde, V. and Lenz, O. K.: The early Eocene of Schöningen (N-Germany) - an interim report, *Austrian Journal of Earth Sciences*, 105(1), 88–109, 2012.
- Röhl, U., Brinkhuis, H., Stickley, C. E., Fuller, M., Schellenberg, S. A., Wefer, G. and Williams, G. L.: Sea Level and Astronomically Induced Environmental Changes in Middle and Late Eocene Sediments from the East Tasman Plateau, in *The Cenozoic Southern Ocean: Tectonics, Sedimentation, and Climate Change Between Australia and Antarctica*, edited by N. F. Exon, J. P. Kennett, and M. J. Jone, pp. 127–151, American Geophysical Union. [online] Available from: <http://onlinelibrary.wiley.com/doi/10.1029/151GM09/summary> (Accessed 17 November 2015), 2004.
- 15 Sangiorgi, F., Dinelli, E., Maffioli, P., Capotondi, L., Giunta, S., Morigi, C., Principato, M. S., Negri, A., Emeis, K.-C. and Corselli, C.: Geochemical and micropaleontological characterisation of a Mediterranean sapropel S5: A case study from core BAN89GC09 (south of Crete), *Palaeogeography, Palaeoclimatology, Palaeoecology*, 235(1–3), 192–207, doi:10.1016/j.palaeo.2005.09.029, 2006.
- 20 Scher, H. D. and Martin, E. E.: Circulation in the Southern Ocean during the Paleogene inferred from neodymium isotopes, *Earth and Planetary Science Letters*, 228(3), 391–405, doi:10.1016/j.epsl.2004.10.016, 2004.
- Schouten, S., Hopmans, E. C., Schefuß, E. and Sinninghe Damsté, J. S.: Distributional variations in marine crenarchaeotal membrane lipids: a new tool for reconstructing ancient sea water temperatures?, *Earth and Planetary Science Letters*, 204(1–2), 265–274, doi:10.1016/S0012-821X(02)00979-2, 2002.
- 25 Schouten, S., Hugué, C., Hopmans, E. C., Kienhuis, M. V. M. and Sinninghe Damsté, J. S.: Analytical Methodology for TEX86 Paleothermometry by High-Performance Liquid Chromatography/Atmospheric Pressure Chemical Ionization-Mass Spectrometry, *Anal. Chem.*, 79(7), 2940–2944, doi:10.1021/ac062339v, 2007.
- 30 Sijp, W. P., England, M. H. and Huber, M.: Effect of the deepening of the Tasman Gateway on the global ocean, *Paleoceanography*, 26(4), PA4207, doi:10.1029/2011PA002143, 2011.
- Sijp, W. P., von der Heydt, A. S., Dijkstra, H. A., Flögel, S., Douglas, P. M. J. and Bijl, P. K.: The role of ocean gateways on cooling climate on long time scales, *Global and Planetary Change*, 119, 1–22, doi:10.1016/j.gloplacha.2014.04.004, 2014.
- 35 Sijp, W. P., von der Heydt, A. S. and Bijl, P. K.: Model simulations of early westward flow across the Tasman Gateway during the early Eocene, *Clim. Past*, 12(4), 807–817, doi:10.5194/cp-12-807-2016, 2016.



- Sluijs, A. and Brinkhuis, H.: A dynamic climate and ecosystem state during the Paleocene-Eocene Thermal Maximum: inferences from dinoflagellate cyst assemblages on the New Jersey Shelf, *Biogeosciences*, 6(8), 1755–1781, doi:10.5194/bg-6-1755-2009, 2009.
- 5 Sluijs, A., Brinkhuis, H., Stickley, C. E., Warnaar, J., Williams, G. L. and Fuller, M.: Dinoflagellate cysts from the Eocene–Oligocene transition in the Southern Ocean: results from ODP Leg 189, in *Proc. ODP, Sci. Results*, 189, pp. 1–42, College Station, TX (Ocean Drilling Program), 2003.
- Sluijs, A., Pross, J. and Brinkhuis, H.: From greenhouse to icehouse; organic-walled dinoflagellate cysts as paleoenvironmental indicators in the Paleogene, *Earth-Science Reviews*, 68(3–4), 281–315, doi:10.1016/j.earscirev.2004.06.001, 2005.
- 10 Sluijs, A., Brinkhuis, H., Williams, G. L. and Fensome, R. A.: Taxonomic revision of some Cretaceous–Cenozoic spiny organic-walled peridiniacean dinoflagellate cysts, *Review of Palaeobotany and Palynology*, 154(1–4), 34–53, doi:10.1016/j.revpalbo.2008.11.006, 2009.
- Sluijs, A., Bijl, P. K., Schouten, S., Röhl, U., Reichart, G.-J. and Brinkhuis, H.: Southern ocean warming, sea level and hydrological change during the Paleocene-Eocene thermal maximum, *Clim. Past*, 7(1), 47–61, doi:10.5194/cp-7-47-2011, 15 2011.
- Sluijs, A., Zeebe, R. E., Bijl, P. K. and Bohaty, S. M.: A middle Eocene carbon cycle conundrum, *Nature Geosci*, 6(6), 429–434, doi:10.1038/ngeo1807, 2013.
- Spofforth, D. J. A., Agnini, C., Pälke, H., Rio, D., Fornaciari, E., Giusberti, L., Luciani, V., Lanci, L. and Muttoni, G.: Organic carbon burial following the middle Eocene climatic optimum in the central western Tethys, *Paleoceanography*, 20 25(3), doi:10.1029/2009PA001738, 2010.
- Stacey, A., Mitchell, C., Nayak, G., Struckmeyer, H., Morse, M., Totterdell, J. and Gibson, G.: Geology and petroleum prospectivity of the deepwater Otway and Sorell basins: new insights from an integrated regional study, *The APPEA Journal*, 51(2), 692–692, doi:10.1071/AJ10072, 2013.
- 25 Stickley, C. E., Brinkhuis, H., McGonigal, K. L., Chaproniere, G. C. H., Fuller, M., Kelly, D. C., Nürnberg, D., Pfuhl, H. A., Schellenberg, S. A., Schoenfeld, J., Suzuki, N., Touchard, Y., Wei, W., Williams, G. L., Lara, J. and Stant, S. A.: Late Cretaceous–Quaternary biomagnetostratigraphy of ODP Sites 1168, 1170, 1171, and 1172, *Tasmanian Gateway*, edited by N. F. Exon, J. P. Kennett, and M. J. Malone, pp. 1–57, Ocean Drilling Program, College Station, TX., 2004a.
- 30 Stickley, C. E., Brinkhuis, H., Schellenberg, S. A., Sluijs, A., Röhl, U., Fuller, M., Grauert, M., Huber, M., Warnaar, J. and Williams, G. L.: Timing and nature of the deepening of the Tasmanian Gateway, *Paleoceanography*, 19(4), PA4027, doi:10.1029/2004PA001022, 2004b.
- Stover, L. E. and Partridge, A. D.: Tertiary and Late Cretaceous spores and pollen from the Gippsland Basin, southeastern Australia, *Proceedings of the Royal Society of Victoria*, 85(2), 237–286, 1973.
- 35 Sutherland, R., Collot, J., Bache, F., Henrys, S., Barker, D., Browne, G. H., Lawrence, M. J. F., Morgans, H. E. G., Hollis, C. J., Clowes, C., Mortimer, N., Rouillard, P., Gurnis, M., Etienne, S. and Stratford, W.: Widespread compression associated with Eocene Tonga-Kermadec subduction initiation, *Geology*, 45(4), 355–358, doi:10.1130/G38617.1, 2017.
- Sutherland, R., Dickens, G. R., Blum, P., Agnini, C., Alegret, L., Bhattacharya, J., Bordenave, A., Chang, L., Collot, J., Cramwinckel, M. J., Dallanave, E., Drake, M. K., Etienne, S. J. G., Giorgioni, M., Gurnis, M., Harper, D. T., Huang, H. H. M., Keller, A. L., Lam, A. R., Li, H., Matsui, H., Newsam, C., Park, Y. H., Pascher, K. M., Pekar, S. F., Penman, D. E.,





- Saito, S., Stratford, W. R., Westerhold, T. and Zhou, X.: Tasman frontier subduction initiation and paleogene climate, Integrated Ocean Drilling Program: Preliminary Reports, doi:<http://dx.doi.org/10.14379/iodp.pr.371.2018>, 2018.
- Taylor, D. J.: Biostratigraphic Log - Latrobe No.1 Bore, 1964.
- 5 Taylor, K. W. R., Huber, M., Hollis, C. J., Hernandez-Sanchez, M. T. and Pancost, R. D.: Re-evaluating modern and Palaeogene GDGT distributions: Implications for SST reconstructions, *Global and Planetary Change*, 108, 158–174, doi:[10.1016/j.gloplacha.2013.06.011](https://doi.org/10.1016/j.gloplacha.2013.06.011), 2013.
- Thomas, D. J., Bralower, T. J. and Jones, C. E.: Neodymium isotopic reconstruction of late Paleocene–early Eocene thermohaline circulation, *Earth and Planetary Science Letters*, 209(3–4), 309–322, doi:[10.1016/S0012-821X\(03\)00096-7](https://doi.org/10.1016/S0012-821X(03)00096-7), 2003.
- 10 Thomas, M. K., Kremer, C. T., Klausmeier, C. A. and Litchman, E.: A Global Pattern of Thermal Adaptation in Marine Phytoplankton, *Science*, 338(6110), 1085–1088, doi:[10.1126/science.1224836](https://doi.org/10.1126/science.1224836), 2012.
- Tickell, S. J., Abele, C. and Parker, G. J.: Palynology of the Eastern Otway Basin, Geological Survey of Victoria Unpublished Report, (1993/18), 1993.
- Torsvik, T. H., Van der Voo, R., Preeden, U., Mac Niocaill, C., Steinberger, B., Doubrovine, P. V., van Hinsbergen, D. J. J., Domeier, M., Gaina, C., Tohver, E., Meert, J. G., McCausland, P. J. A. and Cocks, L. R. M.: Phanerozoic polar wander, palaeogeography and dynamics, *Earth-Science Reviews*, 114(3–4), 325–368, doi:[10.1016/j.earscirev.2012.06.007](https://doi.org/10.1016/j.earscirev.2012.06.007), 2012.
- Totterdell, J. M., Blevin, J. E., Struckmeyer, H. I. M., Bradshaw, B. E., Colwell, J. B. and Kennard, J. M.: A new sequence framework for the Great Australian Bight: starting with a clean slate, *The APPEA Journal*, 40(1), 95–118, doi:[10.1071/aj99007](https://doi.org/10.1071/aj99007), 2000.
- 20 Villa, G., Fioroni, C., Pea, L., Bohaty, S. and Persico, D.: Middle Eocene–late Oligocene climate variability: Calcareous nannofossil response at Kerguelen Plateau, Site 748, *Marine Micropaleontology*, 69(2), 173–192, doi:[10.1016/j.marmicro.2008.07.006](https://doi.org/10.1016/j.marmicro.2008.07.006), 2008.
- Warnaar, J., Bijl, P. K., Huber, M., Sloan, L., Brinkhuis, H., Röhl, U., Sriver, R. and Visscher, H.: Orbitally forced climate changes in the Tasman sector during the Middle Eocene, *Palaeogeography, Palaeoclimatology, Palaeoecology*, 280(3–4), 25 361–370, doi:[10.1016/j.palaeo.2009.06.023](https://doi.org/10.1016/j.palaeo.2009.06.023), 2009.
- Weijers, J. W. H., Schouten, S., Spaargaren, O. C. and Sinninghe Damsté, J. S.: Occurrence and distribution of tetraether membrane lipids in soils: Implications for the use of the TEX86 proxy and the BIT index, *Organic Geochemistry*, 37(12), 1680–1693, doi:[10.1016/j.orggeochem.2006.07.018](https://doi.org/10.1016/j.orggeochem.2006.07.018), 2006.
- 30 Weijers, J. W. H., Lim, K. L. H., Aquilina, A., Sinninghe Damsté, J. S. and Pancost, R. D.: Biogeochemical controls on glycerol dialkyl glycerol tetraether lipid distributions in sediments characterized by diffusive methane flux, *Geochem. Geophys. Geosyst.*, 12(10), Q10010, doi:[10.1029/2011GC003724](https://doi.org/10.1029/2011GC003724), 2011.
- White, J.: Composite Well Log Latrobe No.1 Water Bore, Department of Mines of Victoria, Melbourne, 1963.
- Williams, G. L., Fensome, R. A. and MacRae, R. A.: The Lentin and Williams Index of Fossil Dinoflagellates 2017 Edition. [online] Available from: <https://palynology.org/wp-content/uploads/2017/01/AASP-Contribution-Series-No.48.pdf>, 2017.



Williams, S. E., Whittaker, J. M., Halpin, J. A. and Müller, R. D.: Australian-Antarctic breakup and seafloor spreading: Balancing geological and geophysical constraints, *Earth-Science Reviews*, 188, 41–58, doi:10.1016/j.earscirev.2018.10.011, 2019.

5 Wrenn, J. H. and Beckman, S. W.: Maceral, Total Organic Carbon, and Palynological Analyses of Ross Ice Shelf Project Site J9 Cores, *Science*, 216(4542), 187–189, doi:10.1126/science.216.4542.187, 1982.

Wrenn, J. H. and Hart, G. F.: Paleogene dinoflagellate cyst biostratigraphy of Seymour Island, Antarctica, *Geological Society of America Memoirs*, 169, 321–448, doi:10.1130/MEM169-p321, 1988.

Zachos, J. C., Dickens, G. R. and Zeebe, R. E.: An early Cenozoic perspective on greenhouse warming and carbon-cycle dynamics, *Nature*, 451(7176), 279–283, doi:10.1038/nature06588, 2008.

10 Zhang, Y. G., Zhang, C. L., Liu, X.-L., Li, L., Hinrichs, K.-U. and Noakes, J. E.: Methane Index: A tetraether archaeal lipid biomarker indicator for detecting the instability of marine gas hydrates, *Earth and Planetary Science Letters*, 307(3–4), 525–534, doi:10.1016/j.epsl.2011.05.031, 2011.

15 Zinsmeister, W. J.: Biogeographic significance of the late Mesozoic and early Tertiary molluscan faunas of Seymour Island (Antarctic Peninsula) to the final breakup of Gondwanaland, in *Historical Biogeography, Plate Tectonics, and the Changing Environment*, edited by J. Gray and A. J. Boucot, pp. 349–355, Oregon State University, Corvallis., 1979.

Zwiep, K. L., Hennekam, R., Donders, T. H., van Helmond, N. A. G. M., de Lange, G. J. and Sangiorgi, F.: Marine productivity, water column processes and seafloor anoxia in relation to Nile discharge during sapropels S1 and S3, *Quaternary Science Reviews*, 200, 178–190, doi:10.1016/j.quascirev.2018.08.026, 2018.